Semiconductor Metal Oxide Nanocomposite for Environmental Clean Up

By:

Qaisar Abbas Shafqat

30-FBAS/MSPHY/F10

Supervised By:

Dr. Shamaila Sajjad

Assistant Professor

DEPARTMENT OF PHYSICS

Faculty of Basic and Applied Sciences

INTERNATIONAL ISLAMIC UNIVERSITY,

ISLAMABAD

(2012)

1. Semiconductors ; Optical properties

2. Semiconductors ; Physics

DEPARTMENT OF PHYSICS

FACULTY OF BASIC AND APPLIED SCIENCES

INTERNATIONAL ISLAMIC UNIVERSITY

ISLAMABAD, PAKISTAN

2012

Semiconductor Metal Oxide Nanocomposite for Environmental Clean Up

By

Qaisar Abbas Shafqat

(30-FBAS/MSPHY/F10)

This thesis is submitted to Department of Physics, International Islamic University Islamabad for the award of MS Physics Degree.

Signature:----------

(Chairman, Dept. of Physics)

Signature:---------- DEAN Faculty of Basic & Applied Science International Islamic University Islamabad

(Dean FBAS, IIU, Islamabad)

Dated: 11 September, 2012

Final Approval

It is certified that the work presented in this thesis entitled "*Semiconductor Metal Oxide Nanocomposite for Environmental Clean Up*" by **Qaisar Abbas Shafqat**, **Registration No. 30-FBAS/MSPHY/F10** is of sufficient standard in scope and quality for the award of degree of MS Physics from International Islamic University, Islamabad.

Committee

External Examiner

Dr. Nazar Abbas Shah
Associate Professor,
Department of Physics, COMSATS,
Islamabad.

Internal Examiner

Dr. Waqar Adil Syed
Chairman,
Department of Physics (FBAS)
International Islamic University, Islamabad

Supervisor

Dr. Shamaila Sajjad
Assistant Professor,
Department of Physics (FBAS)
International Islamic University, Islamabad

Co-Supervisor

Dr. Sajjad Ahmed Khan Leghari
Senior Scientist, PAEC Islamabad.

A thesis submitted to

Department of Physics

Faculty of Basic and Applied Sciences

International Islamic University Islamabad

as a partial fulfillment for the award of the degree of

MS Physics (Nanotechnology)

Declaration

I hereby declare that this thesis work, neither as a whole nor a part of it has been copied out from any source. Further, work presented in this dissertation has not been submitted in support of any application for any other degree or qualification to any other university or institute. If any part of this project is proved to be copied from any source or found to be reproduction of some other project, I shall be legally responsible for punishment under the plagiarism rules of Higher Education Commission (HEC), Pakistan.

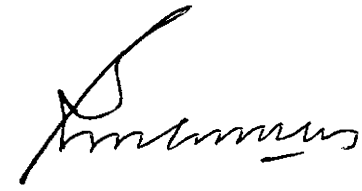

Qaisar Abbas Shafqat

(30-FBAS/MSPHY/F10)

Papers for Publications

1. Qaisar Abbas Shafqat, Dr. Shamaila Sajjad, Dr. Sajjad Ahmed Khan Leghari, Dr. Syed Waqar Adil, Study of mesoporous Fe_2O_3/TiO_2 nanocomposite as a visible light sensitive material. Submitted in Journal of Chemical Physics Letter.

Dedicated to;

The Souls of my Beloved Parents,

(Ghulam Haider & Shamshad Begam)[late]

My Wife Nazia,

My Son Muhammad Irtaza Abbas

And

My Daughter Farwa Abbas

ACKNOWLEDGEMENTS

First of all, I am thankful to Almighty Allah, for His kind blessing upon me who provide the opportunity to work in this field and empowered and blessed wisdom to work and plan with devotion. I am also thankful to my beloved Holy Prophet Muhammad (Peace be upon him) who is forever a model of guidance and knowledge for humanity.

I would like to thank Dr. Shamaila Sajjad (Supervisor) and Dr. Sajjad Ahmad Khan Leghari (Co-supervisor) for their support, guidance, encouragement, and advice that they have always graciously provided me over the past one year. Simply stated, they are the best advisors that I could have asked for. I also would like to thank Dr. Syed Waqar Adil, Chairman, Dr. Javed Iqbal Saggu, Assistant Professor, Dr. Muhammad Fakhar-e-Alam, Assistant Professor, Department of Physics, International Islamic University, Islamabad, Pakistan for their advices and comments throughout my studies. I particularly want to thank Mr. Aslam Hayat, DG, Mr. Shafqat Moharram , Mr. Shamsuddin , Mr. Abdul Qadir Khan, Dr. Shakeel Abbas Rofi , Mr. Abdul Waheed (Pakistan Atomic Energy Commission) for encouragement, and most importantly friendly atmosphere that they always generously offered, without which this project would not possible. I am very grateful to Dr. Muhammad Anees-ur Rehman, incharge XRD Labs, Department of Physics COMSATS Institute of Information Technology, Islamabad, Dr. Muhammad Mujahid, Incharge SEM Labs, SCME, NUST, Islamabad provided me from time to time. I would like to thank Dr. Mazhar (PIEAS) for BET surface area. Mr. Javed Iqbal, Electron microscopist, NIBGE, Faisalabad, for TEM facility. I would also like to thank Faisal Zeb (class fellow) for all of his experimental contributions, advice, and time, without which I could not have proceeded. Finally and most importantly, I would also like to thank my friends that I have made in campus and most importantly those who have always been there for me and will always be with me (Insha'Allah)

Qaisar Abbas Shafqat

Table of Contents

List of Figures

List of Tables

List of Abbreviations

■ ***A.R.***	Analytical grade
■ ***CB***	conduction ban
■ ***DRS***	UV-vis absorbance spectra
■ ***D.D***	double distilled
■ ***EtOH***	ethanol
■ ***EDX***	Energy-Dispersive X-ray Spectroscopy
■ e^-	electron
■ E_g	band gap energy
■ ***FT-IR***	Fourier transform infrared spectra
■ ***FWHM***	Full width half maximum
■ h^+	hole
■ $h\nu$	energy
■ ***MO***	methyl orange
■ ***NHE***	normal hydrogen electrode
■ ^-OH	hydroxyl ion
■ $\bullet OH$	hydroxyl radical
■ O_2^-	super oxide
■ ***P-25***	commercial TiO_2 (Degussa) composed of ca. 20 .wt. % rutile and 80 wt. % anatase
■ ***SEM***	Scanning electron microscopy
■ TiO_2	Titania
■ ***TBT***	Tetra butyly titanate
■ ***UV***	ultraviolet radiations
■ ***VB***	valance band
■ ***Vis***	visible irradiations
■ ***WAXRD***	Wide Angle X-ray Scattering
■ ***XRD***	X-ray diffraction spectroscopy
■ λ	wave length
■ θ	Bragg angle

ABSTRACT

Mesoporous titanium oxide (Ms-TiO_2) is synthesized by a combined modified sol–gel and hydrothermal method. Ms-TiO_2 is impregnated with Fe_2O_3 (Iron Oxide) to prepare the different percentages of Fe_2O_3/TiO_2 nanocomposites. The samples are characterized by X-ray diffraction (XRD), UV-vis diffuse reflectance spectroscopy (DRS), Scanning electron microscopy (SEM), Transmission electron microscopy (TEM), BET surface area, Fourier transform infrared spectra (FT-IR) and Energy dispersive X-ray spectroscopy (EDXS) techniques. XRD spectra show that the samples are composed of anatase. UV-vis diffuse reflectance spectroscopy shows an extension of light absorption into the visible region. The photo oxidation efficiency is evaluated by degradation of methyl orange under visible illumination. The samples loaded with 2.0 % of Fe_2O_3 show superior photocatalytic activity and conductivity to Degussa P-25, pure TiO_2 and Fe_2O_3. Due to mesoporous structure andFe_2O_3 photosensitization, the catalyst shows high activity

CHAPTER - 01

1. Introduction

1.1 Nanotechnology

Nanotechnology means that at least one dimensions of the objects are of the order of 10^{-9} m. In nanotechnology we manipulate the structure of the matter on nano scale i.e. from few nanometer to hundreds of nanometers. The concept of nanotechnology was extended and got popularity in 1986. In 1974 Norio Taniguichi [1] was the first person who used the term nano technology to explain the controlling processes of the order of a nanometer, in semiconductors. In the decade of 1980, the scientist, business persons, media groups and other agencies approved the term nanotechnology where the dimensions of matter structure are fabricated and controlled from nanoscale to hundreds of nanometers and have visible effects and new applications. At this small scale, to produce new devices and materials that have useful and extraordinary properties. Only few technologies shows only partially structure control at the nano size, however producing functional products are already in use. These technologies are also being additional developed to manufacture even more refined products in which the structure of matter is more specifically controlled. The foresight nanotechnology challenges focus on applying these developing technologies to solve vital world problems. The suggestion that modern nanotechnology will consist of artificial molecular machine systems able to build a complex systems to atomic precision has been contentious within the scientific society. Generally, proponents are agreed with the theoretical study attached with the existence of multiple completion of reasonable pathways from present technology, while the opponents are not convinced with theoretical view and lack of direct experimental evidence. The advanced nanotechnology based on our present theoretical studies of physics and chemistry and tells us about the systems capability to control the structure of matter at the nano scale. Although the excellent way from present experimental

techniques to build superior systems is not very clear yet. It our proposes improved long-term, cleaner, safer, and smarter products for our homes, for interactions, medicine, transportation, agriculture and for industry in general, that's why it is called general-purpose technology. It has several commercial as well as various military uses—making future more dominant weapons and tools of observation, due to this it is called dual purpose technology.

1.1.1 APPROACHES FOR SYNTHESIS OF NANOMATERIAL

Generally, scientists use two types of approaches for the preparation and manufacturing of nanomaterials as given in Figure 1.1.

1. Bottom-up approach
2. Top-down approach

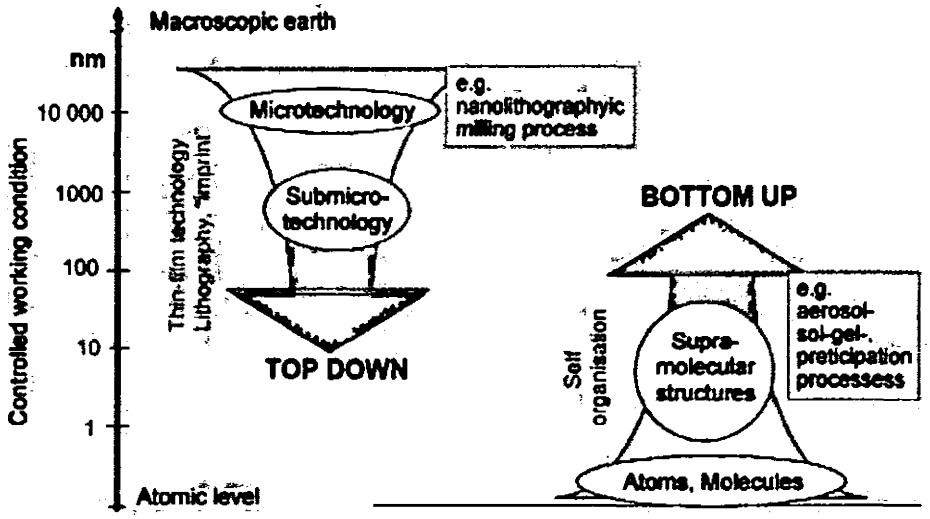

Figure 1.1: Approaches of nanoparticles production.

Bottom-up approach

In this approach scientists uses the smaller of materials, up to atomic scale with additional self-assembly process leading to the formation of nanostructures. At self-assembly stage, the physical forces working at nano scale are used to merge basic

units into bigger stable structures. For examples during the development and formation of quantum dot, epitaxial expansion and formation of nanoparticles from colloidal diffusion.

Top-down approach

This approach uses bigger (macroscopic) as initial structures, which can be able to control the processing of nanostructures. Etching through the mask, ball milling and application of severe plastic deformation are the typical example of this approach, ,.

1.1.2 NANOTECHNOLOGY AND ENVIRONMENTAL SCIENCE

Internationally, the greatest problem faced by the researcher and scientist in 21^{st} century, is *"Environmental pollution"* on a worldwide scale. Many scientists and researchers of this field are discovering new systems for the solution of these problems. Semiconductor metal oxide composite materials can improve the particular applications in reducing the different pollutants in environment. Photocatalytic systems efficiently breaks many unwanted organics compounds by the use of the effective semiconductor metal oxide photo catalysts activated by ultra-violet (UV) radiation. The requirement for visible light sensitive photocatalytic systems has been rising significantly . At present, user friendly and efficient photo catalysts sensitive to the solar spectrum and particularly indoor lighting are needed.

A new horizons have been opened with the invention of materials having nano structure, giving the fresh opportunities to solve the problems in environmental pollution. The higher surface –to-volume ratio of nanoparticles, quantum size effects, and the capability to adjust the surface properties through molecular adjustment to make nanostructures materials ideal for many environmental purification applications. Titanium dioxide (TiO_2) is the most investigated materials for photocatalyst and widely used for many environmental disciplines especially for self-cleaning [2], water purification [3] , sterile[4] and environmental clean up [5]. Moreover, it also acts as

sensors [6], exchanging solar energy[7] and as anti ultraviolet (UV) agent [8]. TiO_2 offer additional benefit of cheaper price, better active photocatalytic, more permanence, toxic free, hydrophilicity and refractive index is high. Scientists are working to modify this material for further professional applications. Honda-Fujishima[9] reported that the photo excited TiO_2 have physically powerful oxidation and reduction capabilities to photoinduce breakdown of water molecule. The initial experiment performed by "Frank and Bard"[10] to check the TiO_2 potential breakdown cyanide molecules in water. This experiment has more importance in environmental sciences. Photocatalytic reactions at the surface of TiO_2 have created more interest in practical usage of environmental cleanup, for example self cleaning of floor covering, glasses, and windows. TiO_2 showed an efficient photocatalyst action for wastewater and polluted air refinement and for automatically clear the surfaces. The modern applications of nanoscale TiO_2 will be used as photocatalysis for chemical degradation and antimicrobial activity in water and air .

Scientists have used this material as a photoanode for segreggation of water to generate energy [9,11-13]. Due to larger energy band gap i.e. 3.2 eV, the photocatalytic action is only accessible under ultraviolet (UV) light i.e. wavelength less then 398nm, which is a tiny part of solar spectrum. Hence, it is needed to build up TiO_2, active in visible range of light to enhance the advantage of solar light for photocatalytic action, for use in environmental refinement.

During the last few years TiO_2 has been extensively used for the synthesizes of different types of nanomaterials such as nanoparticles, nanorods, nanowires, nanotubes, and mesoporous and nanoporous materials [14] . In spite of scale, TiO_2 maintains its photocatalytic abilities, moreover, due to surface reactivity of nano structured TiO_2 , that fosters its interactions with natural organic molecules, such as phosphorylated proteins and peptides [15].

1.1.3 CRYSTAL STRUCTURE OF TiO_2

There are three crystalline forms of TiO_2 exists in environment i.e. anatase, rutile and brookite. The crystal size of all forms are different in each case [16], and only one stable phase of TiO_2 is found, called rutile (tetragonal) and rest are metastable, as specified in Table 1.1.

Table 1.1 Phases of TiO_2

Phase (Reference)	Crystal Structure	a (Å)	b (Å)	c (Å)
Anatase	Tetragonal	13.789	3.789	9.514
Rutile	Tetragonal	4.594	4.594	2.959
Brookite	Orthorhombic	9.166	5.436	5.135
Anatase with corner defects	–	3.96	3.96	2.7

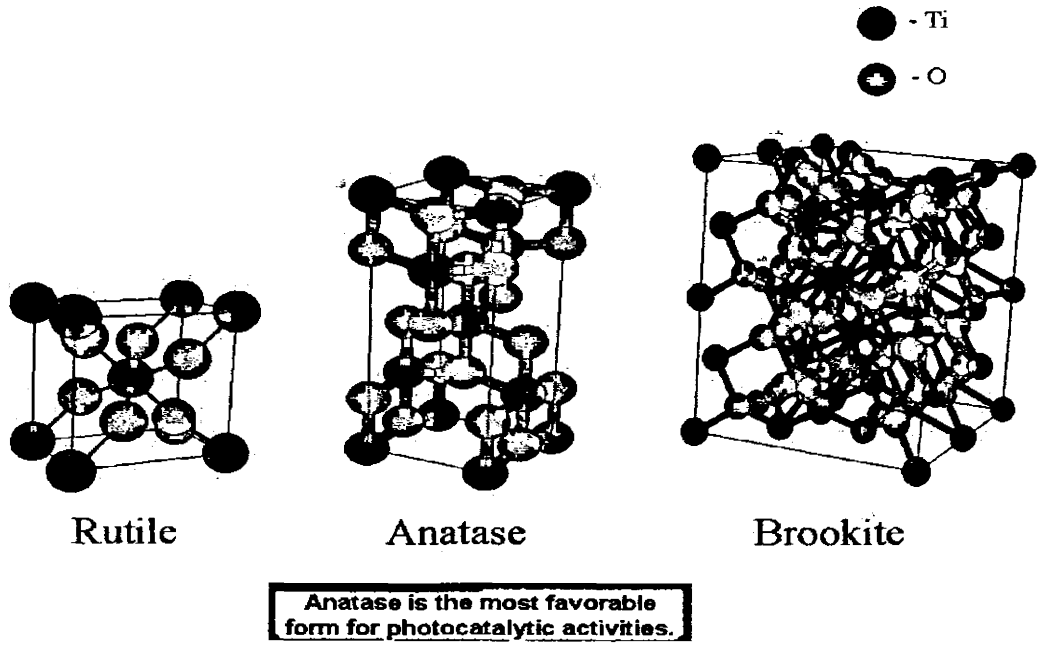

Figure 1.2: Crystal structures of anatase, rutile and brookite TiO_2

Although rutile phased TiO_2 has a large range of applications mostly in the color industry, the band gap energy of anatase is 3.2 eV has verified that TiO_2 has most active crystal structure ,because it has high surface area and its encouraging energy band positions.

1.2 Photo-catalysis

Photo catalysis has become an more important and interesting field and widely investigated topic among the researchers of all fields of science, and is being pursued today to take an ever-increasing problem of environmental pollution. The term "photo catalytic" defined as, the ability of a material to form electron-hole pairs upon absorbing electromagnetic radiation. When a photocatalysts is illuminated with light having energy $\geq$ band gap energy, the electrons in the valance band are excited to conduction band, leaving holes behind in valance band.

$$\textbf{Photocatalysts (e.g., } TiO_2\textbf{)} \xrightarrow{h\upsilon} e_{CB}^{-} + h_{VB}^{+}$$

The excited electron–hole pair recombine and may release the heat energy, without any chemical effect. However, if the charge carriers reaches to the surface of the semiconductor without recombining, they may involve in various oxidation and reduction reactions with the absorbed species such as water, oxygen and other organic and inorganic matters. These oxidation and reduction reactions are the basic mechanism for photocatalysts. A simple photocatalysts mechanism of semiconductor upon UV and visible irradiations is shown in Figure 1.3 [17].

The term photocatalysis is being used since 1920s, although the name itself has drawn analysis since it incorrectly implies a catalytic reaction driven by light. However, mostly, it defines a photoreaction accelerated in the presence of a catalyst. The semiconductors are usually selected as photocatalysts, due to the small energy gap sandwiched between the valence and conduction bands. For purpose of active photocatalysis to carry on, the semiconductors require to take up energy equivalent or greater to its band energy. Then electron - hole pairs(e^-/h^+) are produced with the movement of electrons.

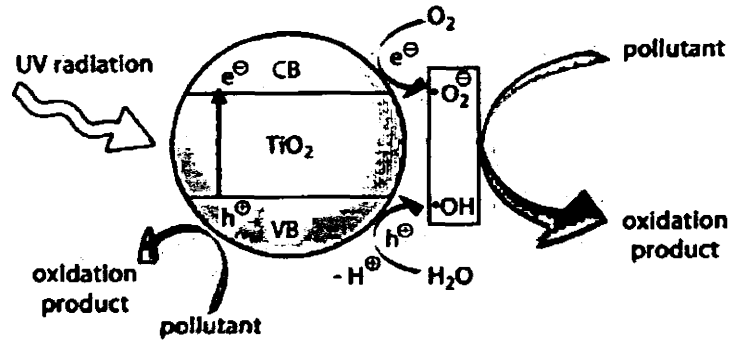

Figure 1.3(a). Photocatalysis mechanism of pure TiO_2 upon UV irradiations.

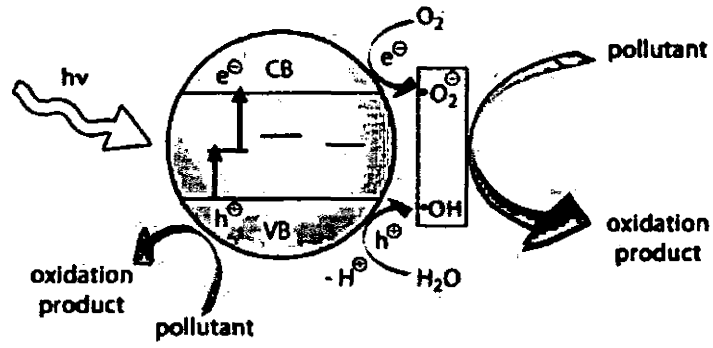

Figure 1.3(b). Photocatalysis mechanism of doped TiO_2 upon irradiations with visible light.

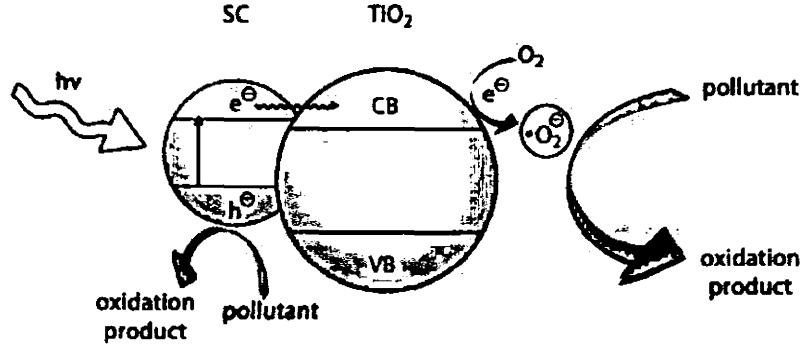

Figure 1.3(c). Photocatalysis mechanism of sensitized TiO_2 upon irradiations with visible light.

Anatase structured TiO_2 is supposed to be an energetic photocatalytic module depending upon electron-hole interaction, chemical characteristics and action of photo-catalytic for breaking down the organic compounds. This shows that surface

band bending characteristics that is formed the strong upward band bending(Figure 1.4) [18]. On the other hand, massive interaction of electrons and holes were taken place in rutile TiO_2, as a result, holes are extremely near to the surface are attentive and move into the surface.

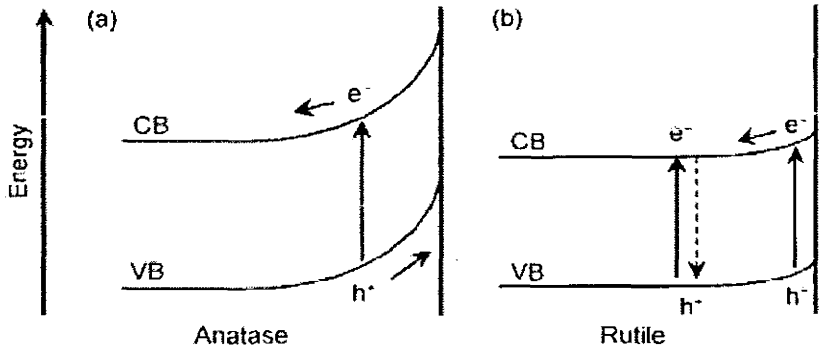

Figure 1.4 Bending of surface band of TiO_2[18]

The photocatalytic process itself does not going to change; however, a new generation of photocatalysts must be created to utilize the available solar spectrum and not merely the scarcely available UV spectrum. This is a relatively recent objective that has been intensively investigated during the past decade although the interest in the field has been increasing rapidly as can be seen by the numbers of papers, books, conferences and available applications that are being devoted to the topic. Visible light photocatalysis is currently being pursued across the globe, including research groups from countries such as Japan, China, France, South Korea, United States, United Kingdom, Germany, Canada, Italy and Taiwan, among others, the current success of these photocatalysts is limited.

Most of the modern work in semiconductor photochemistry took place in 1960s, leading to the first photo electro chemical cell for splitting water, using TiO_2 and Pt coated electrodes in early 1970s [9]. In early 1980s, TiO_2 was used for the first time to activate the reactions in the photo mineralization of selected organics. Since that time, research in the field of photo catalysis has been dominated by studies on the photo ca-

talytic oxidation of organic compounds in water, although there is an increasing interest in oxidizing bacteria and volatile organic chemicals for the purpose of air purification. Over the years, for air purification many semiconductors with photocatalytic properties have been either thoroughly or partially prepared [19-20].

1.3 Modifications of TiO_2

1.3.1 Modifying with Charge-Transfer Catalysts

Charge-transfer catalysts (CTCs) are molecules that have the capability to trap reactive electrons (e^-) and electropositive holes (h^+). In case of TiO_2, the addition of a CTC to the nanoparticle allows more effectively trapping of electropositive holes on the surface of hydroxyl sites of TiO_2 molecule. The enhanced trapping capability of the nanocomposites decreases the rate of charge recombination in TiO_2 and leads to an overall increase in photocatalytic activity. Al_2O_2 and SiO_2 are the most commonly used CTCs with TiO_2 [21] .

1.3.2 Coating with Photosensitizing Dyes

The process of coating creates nanoconjugates rather than nanocomposites ; however, these mixed structures often have enhanced photocatalytic abilities compared to the bare nanoparticles. The principal focus of adding a photosensitizing dye to a nanoparticle is most often to change the photoresponse of the TiO_2 nanoparticle. For example, alizarin can lower the photon energy required to excite the nanoparticles, thus decreasing the band gap energy of alizarin - coated TiO_2 nanoparticles to 1.4 eV, in the white light range [22]. Konovalova et al [23] have proved by calculation, when carotenoids added to TiO_2, it formed ROS on the surface of nanoconjugates under red light irradiation.

1.3.3 Noble Metal Deposition or Coupling

Generally a noble metal is defined as an element that has oxidation resistance, even at elevated temperatures. Ruthenium (Ru), Rhodium (Rh), Palladium (Pd), Silver (Ag), Osmium(Os), Iridium(Ir), Platinum(Pt) and Gold(Au) are some of nobel metals, among these, the majority of researcher used gold and silver for the combination with

TiO_2 nanoparticles. Since the noble metals are resistant to oxidation, these are thought to act as an electron sink, promoting the movement of reactive electrons away from the TiO_2 molecule onto the surface of the noble metal [24]. Li and his colleagues [25] have shown that Ag-deposited TiO_2 anatase nanoparticles have a better photoresponse as compared to that of anatase TiO_2 nanoparticles, Degussa P25 TiO_2 nanoparticles, and mixed anatase-rutile TiO_2 nanoparticles. The use of nanocomposite films made by Ag and TiO_2 have been considered to have an improved photocatalytic reactivity compared to the nonmodified material [26]. The deposition of Au and Pt onto TiO_2 nanoparticles has also showed an improvement in the photocatalytic reactivity of TiO_2. Yu and coworkers [27] have reported an improved photocatalytic reactivity of nanocomposite microspheres made with Au and TiO_2 compared to TiO_2 microspheres and Degussa P25 TiO_2 nanoparticles. In addition, UV-illuminated TiO_2 nanofilms embedded with gold nanostructures have better photonic efficiency than UV-illuminated pure TiO_2 films [26].

1.3.4. Cations Doping

In a semiconductor, an extra energy levels can be created by introduction of transition metal ions. From the available energy levels, electron requires lower photon energy to move into the conduction band than the states of unchanged semiconductor. Various transition metals has been doped with TiO_2 [28] , electron paramagnetic resonance was used to examined the results of TiO_2 doped with transition metals such as Mo, Fe and V [29]. Methodical study was carried out for the photo reactivity of TiO_2 when it was doped with 20 different types of metal ions [30]. Photochemical reactivity of TiO_2 was significantly improved when TiO_2 was doped with Ru, Fe, Mo, V, Re and Os. The unfavorable photocatalytic activity due to transition metal ions doped TiO_2 may occur due to formation of incomplete d-states in the band gap of TiO_2 [31]. Trapping sites were generated due to incomplete d - states that catch holes from valence band (VB) and the electrons from conduction band. Chemical analysis showed imperfection sites like Ti^{3+} in the lattice of semiconductor with the doping of

TiO_2, whereas the rate of oxidation of Ti^{4+} is very slow as compared to Ti^{3+}. The changes in transmission distance and time of the minority carriers caused the photoactivity [32]. For most excellent separation of electron-holes pairs, potential drop level between the layer of space-charge should always be greater then 0.20 V [33]. Recombination rate of e^-/h^+ directly depends upon dopant content [34]. Fe doped TiO_2 showed a better photocatalytic activity when the doping level of Fe^{3+} is low and less at high doping level of Fe^{3+}, the best content ratio of Fe to Ti is 0.03 mol [35]. Nanorods of pure TiO_2 were synthesized by a conservative alkaline hydrothermal process, these TiO_2 nanorods were used in preparation of zero valent Fe-doped TiO_2 nanorods [36]. These Fe-doped nanorods were examined in UV light and their photocatalytic degradation efficiency were calculate. These Fe-doped TiO_2 nanorods were showed very high photoactivity as compared with Degussa P-25. Nanoparticles of pure and Fe-doped TiO_2 were prepared with sol-gel method and cured hydrothermally[37]. Trichlorophenol (2,4,6) was degraded oxidatively by Fe-doped TiO_2 which reported a better photocatalytic activity then pure and commercially synthesized TiO_2.

Hydrothermal ion exchange method was used by Khan et al. [38] for synthesized ruthenium doped TiO_2 nanotubes. The resultant photocatalyst was more energetic under visible light, the methylene blue degradation showed that it has more than 80% photocatalytic activity as compared with undoped nanotubes. Prasad et al. [39] investigated the modified TiO_2 nanotubes for sulfur mustard decontaminant, i.e. a lethal chemical fighting mediator. Decontamination reactions were performed at normal temperature. To achieve the high hydrolysis rate of sulfur mustard, TiO_2 nanotubes were doped with Ag^+ rather then doped with Ru^{3+}, Ni^{2+}, Cu^{2+}, Mn^{2+} and Co^{2+}.

TiO_2 nanoparticles doped with Sm^{3+}, La^{3+}, Nd^{3+}, Yb^{3+}, Eu^{3+} and Gd^{3+} (lanthanide ions) were prepared with a s ol-gel technique [40]. The results of these doped TiO_2 nano particles showed that only Gd^{3+}-doped TiO_2 samples have small band gap , minimum particle size, maximum surface area as well as pore volume. Photocatalytic

activity of TiO_2 was improved when doped with lanthanide ions as compared with pure TiO_2, moreover, Gd^{3+}-doped TiO_2 found the most efficient photocatalyst. Hollow spheres of Gd doped TiO_2 were prepared using model of carbon spheres which were prepared by hydrothermally [41]. Under visible light degradation of the Brilliant Red with dye reactive was observed and calculates the efficiency of photocatalytic activity of hollow spheres prepared with Gd doped TiO_2. Also Ce-doped TiO_2 nanoparticles and model of carbon spheres were used for synthesizing of Ce-doped TiO_2 hollow spheres [42].

1.3.5. Anions Doping

A lot of investigation had been made for the improvement of TiO_2 for a quick response to visible light, when doping with a variety of anions e.g. S ,N or C as a alternate for oxygen in the TiO_2 structure. In these doped anion TiO_2 photocatalysts, the p states of the doped anion were mixed with the 2p states of O, due to this, valence band boundary shifts towards up, resulting band gap of TiO_2 become narrow. The formations time of recombination centers of metal anions were less as compared to metal cations, so they are more efficient for improving the photocatalytic activity of TiO_2 [43]. The electronic band configuration of TiO_2 having different types of dopants was calculated by Asahi et al. [44]. Its band gap become significantly narrow by nitrogen doping due to the mixing of p state of N with the 2p states of O. Diwald et al. [45] performed a experiment in which nitrogen monoanions was included in a particular crystal of TiO_2, with sputtering of Ar^+/N^{2+} blend then heat treatment at 627°C in very high vacuum environment. In the customized catalyst, O_2 photodesorption showed surprising blue shift as compared with pure crystals of TiO_2.

One-pot hydrothermal method was used by Ao et al. [46] for preparation of hollow spheres of N-doped TiO_2 using urea as a originator of nitrogen . The degrading rate of Brilliant Red with reactive dye under visible light showed the capability of photocatalytic activity of spheres and was found very high as compared with the hollow spheres of pure TiO_2 and Degussa P25 . Dong et al. [47] were prepared the

array of N-doped TiO_2 nanotube at 500°C, these array of TiO_2 nanotubes were annealing anodized with ammonia. The array of N-doped TiO_2 nanotube showe improved photocatalytic effectiveness of methyl orange degradation in visible light irradiation as compared with undoped nanotubes due to narrow band gap cause by nitrogen doping .

High photocatalytic activity and acetone oxidation was calculated in F - doped TiO_2 by Yu et al. [48] into CO_2 as compared to undoped TiO_2. Many research articles have reported that C-doped TiO_2 is also extremely efficient in reactions as a catalysts. Sakthivel and Kisch [49] found five times more photoactivity of C-doped TiO_2 in the way of the degradation of chlorophenol as compared to N-doped TiO_2 by non-natural synthetic illumination. The photocurrent densities of $TiO_{2-x}C_x$ nanotube arrays were calculated [50] and under visible light they found it very high and more effective in splitting of water compared to undoped TiO_2 nanotube arrays.

By using density functional theory, the electronic properties and response of photoactivity of nitrogen and tungsten doped TiO_2 were calculated. In N - doping, 2p states of inaccessible N is over the peak of the valence band causing red shifts within the optical absorption boundary. The band gap get narrow in W-doping, because 5d states of tungsten(W) are below the conduction band, which reduces the transition energy upto 0.2 eV. [43,51-53]

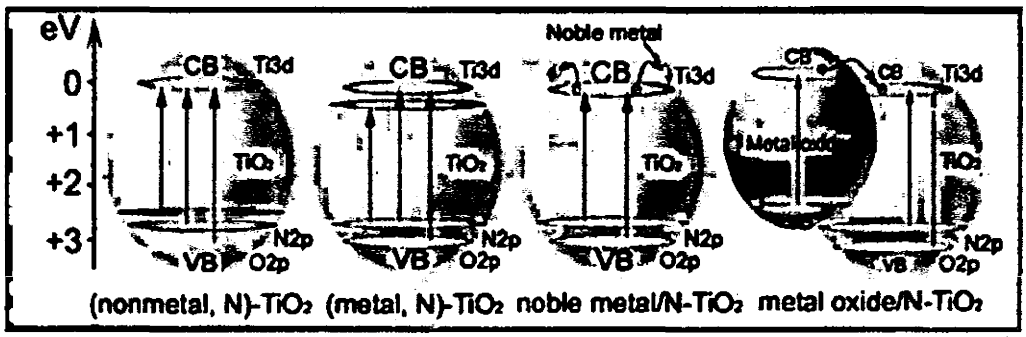

Figure 1.5. Modification of band gap in TiO_2 using metal, non metal, noble metal and metal oxide doping[54]

1.3.6. Co-doping

Charge separation is improved by Co-doping of TiO_2, which is an efficient way.

In Yang et al. [55] report, the TiO_2 was co-doped with 1.0% Fe^{3+} and 0.5% Eu^{3+},which show considerably better photocatalytic activity as compared with undoped TiO_2. Holes were trap by $Fe^{3+}$and electrons were trap by Eu^{3+}, Rates of anion and cation doping was increased by using improve self made charge transfer. In the absorption spectrum of Fe- and Eu-doped TiO_2, red shift occur and which showed better photoactivity for the styrene degradation and phenol photocatalytic oxidation reactions, when it exposed in visible luminosity [56].

TiO_2 nanoparticles co-doped with(Cu, N) were synthesized by Song et al. [57]. They found the amounts of Cu and N for co-doping into TiO_2, which effect on the photocatalytic activity, and increased the absorption upto 590 nm. For the xylenol orange photocatalytic degradation, N and Cu co-doped TiO_2 give better photocatalytic results as compared to undoped N and/or Cu-doped TiO_2. TiO_2 co-doped with Ce and C was prepared by Xu et al.[58] for degradation of Reactive luminous. For nitrobenzene degrade under visible light, N and Ce co-doped TiO_2 photocatalyst was synthesis using sol-gel method [59].

1.3.7. Blending with Metal Oxides

The photoresponse and photocatalytic reactivity were increase when we mix TiO_2 to a narrow - gap semiconductor material . When a coupled TiO_2 nanoparticle with narrow - gap semiconductor is exposed to visible light, then reactive electrons were produced that can pass through the semiconductor and reached to the non activated TiO_2 nanoparticle. The photoactivity of TiO_2 was enhanced near visible light wavelengths with this method. Charge recombination also decreased in TiO_2 coupled with a semiconductor for the reason that the heterojunction gap between the two semiconductors allows for a more well-organized separation of reactive electrons and electropositive holes [60]. CdS, WO_3 and $Cs_xH_{3-x}PW_{12}O_{40}$ are some of generally used semiconductors and metal oxides coupled to TiO_2 [21,60-62].

1.3.8 Modifying with Polymers or Clays

When TiO_2 nanoparticles were functionalized with polymers then they have

excellent conducting properties that capable to away the charged electrons (e^-) and holes (h^+) from the surface of TiO_2. In addition, the mixing of polymers that permit for a large inside boundary area between the polymer and the TiO_2 particle give support in charge separation and also control the charge recombination [63]. In the same way, the addition of clays can give support in charge separation by providing a large inside boundary between the clay and the TiO_2 molecule. In the earlier period, a various combinations of polymer/ TiO_2 nanocomposites have been used on the basis of their capability to improve photocatalytic reactivity. Most practically, polypyrrole, kaolinite, polyaniline, poly amide and poly-lactic acid (PLA) have every one been added to TiO_2 nanoparticles, and each and every one have shown better photocatalytic reactivity of the nanocomposites[63-66]. For example, methyl orange was degraded upto 95.54%

in visible light by polypyrrole-TiO_2 nanocomposites as compared to 40.00% degradation by visible light with pure TiO_2 nanoparticles [63] .

In the same way, Shi - xiong *et al* . verified the capability of UV - and solar light - irradiated aniline methy tri ethoxy silane –TiO_2 nanoparticles composited with polyaniline to enhance the photoresponse and decrease recombination of charges [67]. New methods for preparation of TiO_2 clay nanocomposites have drawn in the use of heterocoagulation to form TiO_2-montmorillonite (MMT) nanocomposites, where in a silicate layer is used to hold the TiO_2 nanoparticle. Kun and coworkers reported that these nanocomposites showed better photocatalytic reactivity than pure TiO_2, due to the extra catalytic activity of the silicate which hold the layer of the nanocomposites [68].

1.4 Comparison of TiO_2 with other photocatalyst materials

The redox potential of a charge couple, is the most important scale for measuring the efficiency of semiconductor photocatalyst, this means that e^-/h^+ lies inside the photocatalysts band gap area. At the base of the conduction band, energy level defined

the dropping ability of photoelectrons while at the peak of the valence band, the energy level determines oxidizing capability of photo generated holes [69]. Figure 1.6 [70] showed the band gap energies of some of commonly used semiconductor photocatalyst. Due to considerable entropy of electron-hole pairs causing from the available transitional states of the movable charges in valence and conduction bands, the free energy of electron-hole pair is lesser as compared to the band gap energy. Apart from having proper band gap energy, the fabrication of perfect semiconductor should also be effortless and uncomplicated to use, price effectual, photo stable, no dangerous for humans and the environment, moreover it should be efficiently respond in sunlight and competent to catalyze the reaction efficiently [69]. The majority of the reported photocatalysts have limitations, for example, in aqueous medium CdS, PbS, and GaAs are not steady suitable for catalysis as they easily under go the photocorrosion and are also harmful [71]. In water ZnO is unsteady because it dissolves rapidly [72] and produced $Zn(OH)_2$ which reside at surface of ZnO particle, which stop the response of the catalyst ultimately. The energy level of the conduction band of WO_3, Fe_2O_3, and SnO_2 were less then reversible potential of hydrogen, therefore the external electrical field is required in a systems that used these materials for water splitting reaction.

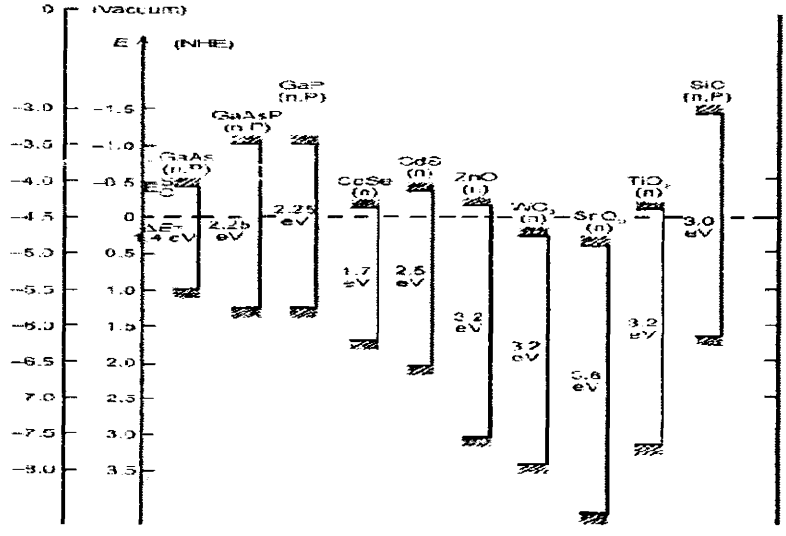

Figure 1.6: Band gap energies of commonly used semiconductors [70].

1.5 Mesoporous Nanostructures

In the present years, manufacturing of hierarchical structured materials are rapidly increasing. For separation and catalysis processes, multiscale pores materials have more attraction. Meanwhile, the diffusion and confinement regimes is required for optimalization [73-76]. Moreover, shape and size selection for guest molecules is much easier in mesopores and micropores materials, due to this we can promot the host-guest interactions. Due to macro channels presence, pore obstruction was avoided because there are much more accessibility of guest molecules for the active sites. Hypothetical results and simulations also confirm that the materials with hierarchical micropores or mesopores shows a better catalytic processes.

There is a experimental challenge for manufacturing of such structures with size control of macroporosity. In this part of work, a simple and new and simple trends adopted for producing materials having mesoporous with interconnecting mesoporous channels. The surface area and size of pore is the most related properties of porous materials. The International Union of Pure and Applied Chemistry (IUPAC) proposed the official classification on the basis of pore diameter[76], which is given in Table 1.2 below.

Table 1.2 Classification of pores according to their diameter or width

Sr. #	Classification of Pores	Pore Size (nm)
1	Micro	< 2
2	Meso	2 – 50
3	Macro	> 50

1.6 Specific Objectives

This MS research work has specific objectives as follows:

1. The design of mesoporous TiO_2 and Fe_2O_3 nanocomposites system having higher photocatalytic and conductive efficiency (both surface properties and quantum yield) in visible light irradiation due to photosensitization of Fe_2O_3 as well as unique mesoporous structure.
2. Preparation of iron incorporated TiO_2 overcome the band gap potential and reduced the electron hole recombination to utilize in environmental cleaning.
3. Photocatalytic efficiency of the produced material is determine and compare with Degussa P25 by degradation of toxic and organic dye pollutants.

CHAPTER - 02

2. Literature Review

This chapter presents the fundamental information's of the research regarding water and air pollutant treatments and photocatalysis processes. The chosen photocatalyst; titanium dioxide (TiO_2), investigation is related to the growth of the photocatalyst and also study is correlated to its performance and activity. Photocatalysis is branch of a group known as Advanced Oxidation Processes (AOP). The group can be divided into three sub-group;

i) HiPox technology, it is chemical oxidation using hydrogen peroxide, ozone and a mixture of both.

ii) UV improved oxidation (UV with ozone, UV with H_2O_2 and UV with TiO_2)

iii) Wet air oxidation with and without catalytic.

The research of Fujishima and Honda[9] have given the birth of present modern photocatalysis. They broke up water molecule into hydrogen and oxygen with a single crystal TiO_2 electrode successfully. In fact, they were working on the production of hydrogen from water but their experiment become the basis of the invention of modern photocatalysis. Many advantages can be obtainable by photocatalysis include:

a) The organic pollutants were completely mineralized with the creation of CO_2, water and mineral acids.

b) Unpreserved reagents are not required for photocatalytic process.

c) energy required to make active the photocatalyst is in the near UV wavelength, making the use of solar energy a possible alternative.

Facchin et al. showed that heterogeneous photocatalysis procedure depends on photon activation of a photocatalyst in easygoing experimental environment i.e. at room temperature and atmospheric pressure. A solid with proper surface physicochemical and electronic properties can work effectively as photocatalyst's,

depending on the reaction under examination. The following things are necessary in any photocatalytic process:

a) a photocatalyst having efficient photon absorption;

b) a large number of photoreduced electron-hole pairs

c) Rate of recombination of these pairs are very low.

A ideal photocatalyst in the scientists interest is titanium dioxide (TiO_2) and other easy to get to photocatalysts are ZnO , CdS and Fe_2O_3. The function of metal doping into nano structred TiO_2 photocatalysts was systematically studied by Choi and co-workers [77]. They arranged many photochemical and photophysical experiments and elaborated the function of metal ion dopant of TiO_2 photocatalysts. The ionic radii of the dopant metal ions were chosen that are similar to Ti^{4+}, as a result, the metal ions were substituted into the lattice of TiO_2 medium would be much easier. Most favorable concentration for all of the dopant existed in the degradation of $CHCl_3$. This work show that, when we doped with Fe^{3+}, Re^{5+}, Mo^{5+}, V^{4+}, Os^{3+}, Ru^{3+} and Rh^{3+} with doping range 0.1-0.5% appreciably raise the photoactivity. The photo response would decrease when doped with Co^{3+} and Al^{3+}. According to Choi et al; the relative effectiveness of a depended on when it served as a intermediary for transferring or recombination of charges. They proved that for useful trapping, dopant played an important role depending on the dopant absorption, energy of dopant in the lattice of TiO_2, their electronic configuration of d state, dopants sharing in the particles, the absorption of donor electron, and the incident light intensity. The metal-doped TiO_2 photoactivity was effected due to improved in interfacial charge transfer in the existence of successful dopants. Fe^{3+}-doped TiO_2 proved that, it is well-organized in the degradation of various types of organic pollutants. The mixing of iron cations can apply physically powerful control on the charge carrier recombination time, and expand the absorption boundary of TiO_2 in visible light.

Using sol-gel process, various Fe^{3+} concentrated doped TiO_2 was synthesis by Xin et al.[78]. They calculated the most favorable dopant concentration. The methods

of photoinduced carriers separation and recombination processes were described as follows:

Fe^{3+}-doped TiO_2 photocatalytic activity was enhanced, when concentration of the dopant substance was less than 0.03 mol%, then photo induced electrons were trapped by Fe^{3+}, that forbidden the recombination of photo induced charges; whereas when the dopant concentration increased by 0.03 mol%, produced Fe_2O_3 which became the recombination centers of photo induced carriers. The level of Fe_2O_3 conduction band is lower and valence band is higher than TiO_2 respectively, Thus, at time of Fe_2O_3 phase creation, the electrons and the holes present in conduction and valence bands of TiO_2 respectively possibly move into Fe_2O_3. This led to the rapid recombination of photo induced electrons and holes.

Microemulsion method was used by Adán et al. [79] for synthesis of Fe-doped TiO_2 and they showed that when Fe^{3+} cations were deposited into TiO_2 structure, an improvement of the photocatalytic activity for the doping intensity up to 1 wt %. They documented the deterioration of photoactivities of elevated iron doping TiO_2 to the elevated levels of surface separation of iron-containing amorphous oxidic phases.

Klosek and Raftery[80] used ambient chemical method for preparation of V-doped TiO_2 photocatalyst. The synthesized photocatalyst was energetic under visible light irradiation, because the visible light excited the vanadium centers and the electrons were transferred into the conduction band of TiO_2.

Cr^{3+} doped TiO_2 was prepared by Anpo and co-workers[81] and reported that the chromium ions efficiently enhanced the photocatalytic activity under visible light. Their study also established the most favorable level of doping concentration. They recognized the improvement of visible-light induced photocatalytic activity to the excitation of 3d electrons of Cr^{3+} which were moved to the conduction band of TiO_2. Lam et al:[82] performed a experiment in which Cr ions was implanted into TiO_2 thin films which were prepared by using sol-gel method. Their results verified that there was a need to manage the quantity of Cr ions in the TiO_2 to obtain well-orga-

nized photocatalytic degradation of formaldehyde vapor.

Venkatachalam et al.[83] prepared Zr^{4+} doped nano- TiO_2 by sol-gel method. However, the mixing of Zr^{4+} in TiO_2 medium caused a large band gap than pure TiO_2, it did delay the growth of grain size, enlarge the surface area, reduce the anatase - rutile phase conversion and speed up the surface hydroxylation. The improvement of absorption of 4-chlorophenol on the surface of catalysts and decrease of the particle size induced by the mixing of Zr^{4+} were responsible for the higher activity of the catalysts. Therefore, the Zr^{4+} doped nano- TiO_2 keep enhanced photocatalytic activity of the degradation of 4chlorophenol than both nano-TiO_2 and commercial Degussa P25.

Mo, Co, Cu, Cr, Fe, W and V (Transition metal ions) doped TiO_2 polycrystalline were synthesized by Di Paola et al [84]. Their work showed that W-doped TiO_2 was the most capable individual for the photodegradation of benzoic acid and 4-nitrophenol. Co-doped TiO_2 was more effective than pure TiO_2 in the degradation of methanoic acid. The environment of the reacting molecules, the acid-base and electronic properties of the photocatalysts were taken into report to make clear the differences of the photoreactivity.

Brezová et al. [85,86] found the photocatalytic breakdown of phenol using TiO_2 photocatalysts doped with metal was prepared by the sol-gel technique on glass fibers. They verified to the photoactivity of doped TiO_2 was powerfully dependent on the nature and absorption of dopant ions. The most excellent results were obtained in terms of phenol breakdown in dopant-free TiO_2, Li^+-, Zn^{2+}-, and Pt-doped TiO_2. The doping of Co^{3+}, Cr^{3+}, Ce^{3+}, Mn^{2+}, Al^{3+}, and Fe^{3+} ions in the TiO_2 photocatalyst had a unfavorable effect on its photocatalytic activity.

Comparison of the photocatalytic properties with and without metal ions dopants of TiO_2 was studied by Bouras et al. [87]. They synthesis Fe^{3+}, Cr^{3+}, and Co^{2+} doped TiO_2 with dopant level ranged in a big domain using sol-gel method. Their work proved that when we introduced Fe^{3+} ions caused the induce energy states

situated within the band gap of TiO_2 , Co^{2+} doping showed a mixed behavior in both doped titania and cobalt titanate; and Cr^{3+} doping caused to the development of an amorphous material by dissolving metal ions. Although, all doped materials they studied showed physically powerful absorption in visible light region, their photocatalytic efficiencies were spoiled as compared to pure TiO_2. The loss of crystallinity or transition from anatase to rutile seemed to explanation for the degradation of photocatalytic properties of doped TiO_2

Anpo et al. [88-90] adopt metal ion-implantation technique to adjust the bulk electronic properties of TiO_2 photocatalysts. Transition metal ions, such as V, Cr, Mn, Fe and Ni, were fixed in the TiO_2 medium. These doped- TiO_2 photocatalysts showed that absorption boundary was shift toward visible light region, which was caused by the high energy implantation process as well as the contact of the transition metal ions with the TiO_2 catalysts, as compared with the metal-doped TiO_2 made by chemical methods

Anpo et al. "claimed that the metal ion-implantation method was an efficient way to retain the photocatalytic properties of TiO_2 under UV irradiation". In metal-doped TiO_2, the metal ions fixed in the TiO_2 medium did not work as electrons and holes recombination centers, but customized its electronic properties. The adjustment of electronic structure of TiO_2 enabled these photocatalysts to absorb and operate efficiently not only under UV but also under visible light irradiation. Nagaveni [91] synthesized W, V, Ce, Zr, Fe, and Cu metal-doped anatase TiO_2 by using solution combustion method. The reduction in the emission intensities may be originated from two reasons: "one was the differences in electronic structure of the metal-doped TiO_2 and the other was the introduction of new defect sites such as oxide ion vacancy". Photocatalytic activity experiments confirmed that the photoactivity of metal-doped TiO_2 was lesser to that of pure TiO_2. This was due to the substituted metal ions behave like recombination centers of the trap sites of electrons and holes and the rate of recombination of electron-hole pairs increased. Computer simulation is a dominant

tool to explain the electronic structures of impurity states at atomic scale. Casarin et al. [92] studied the electronic properties of Nb-doped bulk and surface of rutile TiO_2.by density functional cluster method. Their outcome showed that the electronic structure was considerably disturbed by Nb doping. The control of Nb dopants on the electronic structure was relatively similar to that in the bulk and at the surface of TiO_2 by using DV-X. method,

Nishikawa et al. [93] designed the electronic states of pure and metal-doped (V^{3+} ,V^{4+} ,V^{5+} , Cr^{3+} , Mn^{3+} , Fe^{3+} , Co^{3+} , Ni^{2+} , Ni^{3+}, and Rh^{3+}) anatase and rutile TiO_2 crystals. Their work showed that the band gap is reducing by replacing of Ti^{4+} with metal ions. These outcome were in conformity with the experimental light absorption spectra of which the metal-doped TiO_2 shifted to the visible light region. The reduce of band gap was recognized to the overlap of 3d metal orbitals with 2p orbitals of oxygen ions in TiO_2 and the enlarge in the scale of the covalent bond character between the replacing metal ion and an oxygen ion.

Karvinen et al. [94] used ab initio Hartree-Fock method to calculate the band gap of metal-doped TiO_2. Their results verified that the doping of Ti^{3+},V^{3+} , Cr^{3+}, Mn^{3+} and Fe^{3+} could narrow the band gap of anatase TiO_2. For rutile TiO_2, doping of V^{3+}, Mn^{3+} and Fe^{3+} did not apparently change the band gap. However, Cr^{3+} doping might enlarge the band gap of rutile.

By using ion implantation technique, Yu et al. [95,96] synthesized F-doped TiO_2 by hydrolysis of titanium tetra isopropoxide in a mixed NH_4F-H_2O solution. The F doping not only enhanced the crystal structure of anatase but also covered up the development of brookite phase and controlled the phase transition of anatase to rutile. Absorption spectra proved that the band gap of F-doped TiO_2 was narrower as compared to pure TiO_2 . F-doped TiO_2 showed improved photo-catalytic activity as compared to Degussa P25 when the F to Ti atomic ratios were in the range of 0.5-3 at 500°C.

Yamaki et al. [97] Synthesis F-doped TiO_2 and studies the details about damage

recovery and impurity debate. Their work verified that when the samples were annealed at 300, 600, 1000, and 1200^{0}C for 5 hour TiO_2-xFx along with the recovery of the radiation damage occurred Implanted F atoms could spread to the outer surface together with the recovery of disorder layer. They found the electronic structures of the F-doped TiO_2 by using full-potential linearlized augmented plane wave (FLAPW) method. The replacement of F to O led to a change of the electronic structure around the edge of conduction band of TiO_2. This adjustment could result in a reduction in the efficient band gap by this means inducing visible-light photo-response.

Li et al. [36] prepared Fe-doped TiO_2 nanoparticles using hydrothermal method. Their report showed that when increase in the content of Fe, the photocatalytic activity of Fe-doped TiO_2 decreased. Moreover, XPS results showed that the Fe situated somewhat inside rather than on the outer surface of the samples. They found that, for calculating the photocatalytic characteristics, the Fe position in the crystal structure plays a main role in of the doped samples. Anatase Fe-doped TiO_2 nanoparticles with particles sizes between 10-15 nm were directly synthesized with amorphous TiO_2 nanoparticles and $Fe(NO_3)_3.9H_2O$ by hydrothermal method [98]. A simple method is explained for the preparation of Fe-doped TiO_2 nanoparticles ($Ti_{1-x}Fe_xO_2$) that can be used as a high performance support material for a CO oxidation catalyst. This method give permit to manufacture $Ti_{1-x}Fe_xO_2$ with uniform sizes and shapes. Fe-doped TiO_2 improve the rate of both the release and uptake of oxygen atoms from the catalysts, thus resulting in a high catalytic activity in CO oxidation reactions. These results proved that Au catalyst supported on Fe-doped TiO_2 having 6 atom% Fe dopant showed an outstanding oxidation performance. The results of this report herein represent an innovative way to designing high performance catalysts for oxidation reactions.

At 700°C, using metallorganic chemical vapour deposition technique Fe-doped TiO_2 nano sized particles were prepared. In the reactor, (0.001-0.05)g of ferrocene

amounts used as the basis of Fe - dopant along with titanium originator in order to produce Fe doped TiO_2 nanoparticles with various concentrations. Under luminousand Ultra Violet light, the rate of methylene blue degradation shows the efficiency of photocatalytic activity of Fe-doped TiO_2. The results showed that photocatalytic activity was decreases in Fe doped samples. On the results of X-ray photoelectron spectroscopy (XPS), the non-favorable position of Fe^{3+} in the inner medium of the TiO_2 nanoparticles instead of the outer surface, is a major factor to influence on the photocatalytic performance. [99]

Nano structured (60–70 nm) Fe-doped TiO_2 was produce by a sol-gel method, after that, treatment of freeze-drying upto 2 hours. The outcome show that 0.05g% is the best concentration ratio for Fe-doping in TiO_2 because iron is a crucial ingredient in disturbing the photocatalytic activity. For the curing of paper-making wastewater, less doping concentration of Fe showed higher photocatalytic activity as compared to undoped TiO_2 and 0.05g% Fe concentration found best for photo-degradation effect of paper-making effluent [100].

CHAPTER - 03

3. Experimental Section

3.1 Apparatus and Materials

The materials, reagents, apparatus and instruments used in this thesis work are given in Table 3.1 and 3.2.

Table 3.1 The reagents and materials used in experiment

Reagents	Formula	Specifications
Tetrabutyl titanate	$Ti(OC_4H_9)_4$	A.R
Ferric Nitrate	$Fe(NO_3)_3.9H_2O$	A.R
Ethanol	CH_3CH_2OH	A.R
Polyethylene glycol	$C_{2n+2}H_{4n+6}O_{n+2}$	A.R.
Water	H_2O	D.D.
Methyl Orange	$C_{14}H_{14}N_3NaO_3S$	A.R.
P-25	TiO_2	Degussa

Table 3.2 The reagents and materials used in experiment

Instrument	Manufacturer	Specifications
Mechanical stirrer	-	D-8401
Apparatus drying oven	Memmert Co. Ltd.	600
High temperature Oven	Heraeus Co. Ltd.	D-6450 Hanan Type T5050 EXP
Spectral Filter	-	λ>420 nm
Temperature programmed muffle furnace	Germany NBER	HT16/17 Max.1700 C
Balance	Mettler-Toledo group	AT200,d=0.1mg
Magnetic stirrer	----------	85-1
Ultrasonic machine	Elma Ultrasonic Co. Ltd	1200Hz
Photoreactor Quartz Cell	-	d=2cm,100 mL
Halogen Lamp	-	1000 watt
Centrifugation Machine	-	16000 rpm 50 Hz, 145 Watt
Conductivity meter	DENVER Instrument	Model 250 pH ISE
Electrode	DENVER	K25

3.2 Catalyst Preparation

In the synthesis process, 20 mL TBT was added into the mixture of 20 mL ethanol and 1.0g of PEG (2000) with controlled rate. The mixture was stirred vigorously for 1h. This solution was hydrothermally treated at 120 °C for 12 h followed by filtering and washing for several times with deionized water and ethanol. The samples were dried at 80 °C for 12 h to produce pure TiO_2 and then grind. Samples containing 1.0, 2.0, 3.0 and 4.0 wt. % Fe_2O_3 were prepared by the wet impregnation method. In ethanol solution, TiO_2 and Fe $(NO_3)_3$ were mixed with various molar ratios and placed in agate mortar. After that, at 60°C the mixture was dry upto 1 h, then calcination at 500°C upto 6 h. The notation of prepared samples were given as *x* % Fe_2O_3 over loaded TiO_2, where *x*% denoted Fe/Ti molar ratio.

3.3 Characterization of Catalyst

NIR spectrophotometer of Scan UV-vis is used for getting disperse reflectance spectrum (DRS) of UV-vis, spectrophotometer is prepared with an integrated sphere assembly using $BaSO_4$ as a reflectance sample. For studying the crystallographic properties, X-ray diffraction (XRD) measurements have done with Rigaku apparatus (Cu $K_{\alpha 1}$ radiation, λ = 1.54056 Å) operated at room temperature with 40 kV and 100 mA. For wide angle XRD, 20°-80° angular range was used for recording of diffraction patterns. average crystallite sizes of the samples was estimated with Scherrer equation as given below:

$$D = K\lambda/\beta\cos\theta \qquad \text{(i)}$$

β represent the width of diffraction peak of the anatase(101) at half-height, K is coefficient and equal to 0.89, θ denoted diffraction angle, λ is the wavelength of X-ray related to the Kα radiation of Cu and D represent the average crystal size(in nanometer) of the powder sample. Scanning Electron Microscopy (SEM) (JEOL. JAD-2300) was used for studying the surface morphologies and particle sizes. For electron dispersive X-ray spectrum (EDX) obtained by JEOL (JAD-2300). Transmission electron microscopy (TEM) results were obtained from J E O L

instrument.Micromeritics ASAP 2010 system was used for obtaining adsorption and desorption isotherms of Nitrogen at 77 K. Before the measurement, all the samples were degassed at 473 K. FT-IR spectrometer of manufacturing model Nicolet 740 equipped with beam splitter of KBr along with TGS detector, used for obtaining FT-IR spectra of the samples. To examine the different chemical states of the photocatalysts, Cary 100 UV-vis spectrophotometer was used for recording of UV-vis absorption spectra of the samples.

3.4 Photocatalytic Activity Measurements

The efficiency of Fe_2O_3/TiO_2 nanocomposites photocatalytic was evaluated by the degradation of MO. Under visible and UV light exposure, degradation processes of photocatalytic were studied. 100 mL quartz photochemical reactor was used for performing photo catalytic degradation. The primary concentration of methyl orange in a reaction vessel was kept at 10 mgL^{-1} with a catalyst loading of 0.05 g/50mL. A 1000 W halogen lamp was used as the light source. The short-wavelength components ($\lambda < 420$ nm) of the light were cut off using a cut-off glass filter for visible photoreaction. To preserve the solution at room temperature, a water-cooling arrangement in photochemical reactor, chilled the water-tubes throughout the reaction. Placed lamp at 10 cm from the center of quartz tube. Before illumination, homogenized the reaction mixture by sonicated upto 20 minutes and suspension stirred magnetically in darkness upto 30 minutes to set up adsorption–desorption stability at normal temperature. During irradiation, the suspension of mixture was maintain by stirring. After regular periods, put off the samples and reserved for assessment of photocatalyst. After that mixture was filtered with a millipore filter of 0.22 μm to eliminate the photocatalyst. For MO degradation, the photo activities in dark and under visible light irradiation with and without presence the photo catalyst respectively were also evaluated. From calibration curve, concentration of MO was measured from the peak height at 464 nm. All of the procedure for catalyst measurements were repeated and found the experimental error within ± 0.3%.

3.5 Measurement of Conductivities

The conductivities of solutions are measured by the DENVER Instrument Model 250 pH ISE conductivity meter. The electrode used for conductivity meter is K25/DENVER k=0.547@25C.

CHAPTER - 4

4. Results and Discussion

4.1. X-Ray Diffraction Spectroscopy

Phase configuration, crystal size and crystallinity of TiO_2 participate significant in photocatalytic activity. Different researchers have confirmed that anatase phase of TiO_2 shows higher photocatalytic activity than rutile or brookite phase. The wide angle XRD patterns of pure TiO_2 and different Fe loaded samples calcined at 500 °C are shown in figure 4.1. In Fe_2O_3/TiO_2 nanocomposites samples, diffraction peaks of anatase phase is very large. The characteristic diffractional peaks of anatase around 2θ of 25.3, 38.0, 47.9, 53.9, 55.1, 62.8, 68.9, 70.4, and 75.2 respectively are shown in Figure 4.1.

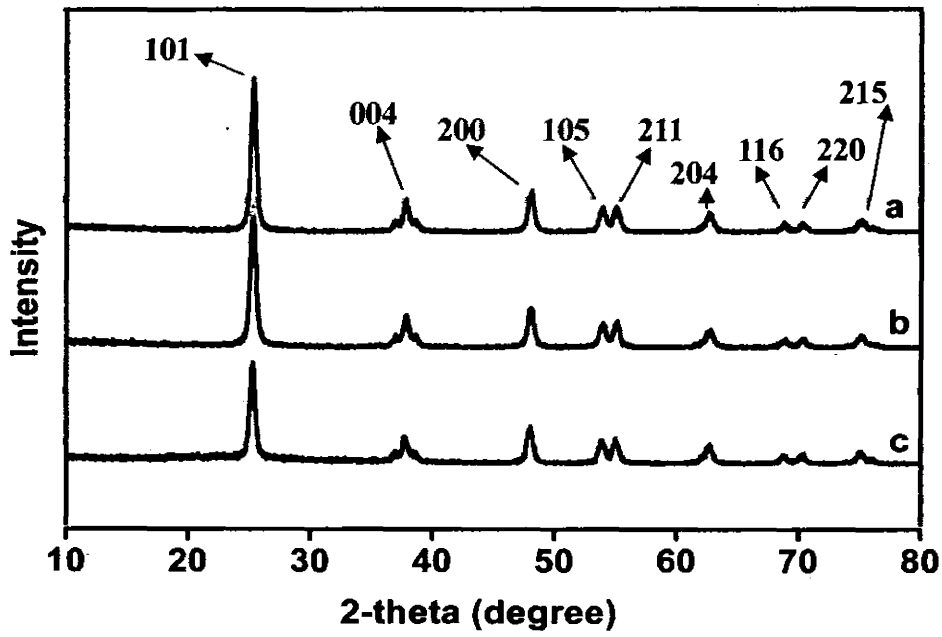

Figure 4.1 XRD patterns of different samples: (a) TiO_2, (b) 2.0% Fe_2O_3/TiO_2, (c) 4.0% Fe_2O_3/TiO_2

No characteristic diffractions of Fe_2O_3 are experimentally found in the nanocomposites samples. The peak widths at 2θ = 25.3 in every composites are very large as compared to undoped TiO_2. Because there is dispersion or amorphous layer of Fe_2O_3 on TiO_2, so the concentration of Fe_2O_3 is very small used for the reveal of

XRD [101,102]. As the contents of Fe_2O_3 increases the peak intensity decreases. The Scherrer equation show that at $2\theta = 25.3$, peak of anatase (101) is become very large which provide the base for prediction of average crystallites size of TiO_2 [103]. The structural study of the Fe_2O_3/TiO_2 with different Fe_2O_3 loading contents confirm the anatase phase and dimension of all the prepared nanoparticles of TiO_2 are 18 –15 nm.

4.2 UV-vis Diffused Reflectance Spectroscopy

The capability of light absorption of the prepared photocatalysts are calculated from spectrum of UV-vis absorption. Spectrum of UV-vis absorption of TiO_2, 2.0 % Fe_2O_3/TiO_2 and 4.0 % Fe_2O_3/TiO_2 samples are shown in figure 4.2, that evidently showed the effectiveness of incorporated Fe_2O_3 on the UV-vis absorption. At 300-380 nm of anatase TiO_2, charge transition in O^{-2}-Ti^{+4} relative to edge take place, due to this effect, we obtained the UV–vis diffuse reflectance spectrum (DRS) of pure TiO_2 sample. These charge transitions show the electrons excitation from valence band to the conduction band. The absorption properties of photocatalysts are highly effected when TiO_2 modified with Fe ions. Within the 450-550 nm range of visible region, 2.0 % Fe_2O_3/TiO_2 composite shows an extra broad and weak absorption(Figure 4.2 b). Further increase in Fe content leads to a linear increase in the absorption band higher than 550 nm in visible region. The Fe^{3+} t_{2g} level is close to the VB of TiO_2; hence, optical transition is expected to occur from Fe t_{2g} to the CB. It induces a larger red-shift and bandgap narrowing thus changing the crystalline and electronic structures [104,105]. Due to narrowing of band gap, the electron is very easily excited from valence band to conduction band. Thus, photocatalytic behavior is different due to narrow band gap and light absorption property. The experimental photocatalytic activity are in excellent consensus with the UV-Vis diffuse reflectance spectra. $E_g = 1239.8/\lambda$ equation is used for calculating the band gap energies (E_g) of the prepared photocatalysts, the wavelength(λ) values related to the common point of the vertical and horizontal parts of the spectra given in Table 4.1.

Table 4.1. Energy band gap of pure TiO_2, 2.0 % Fe_2O_3/TiO_2 and 4.0% Fe_2O_3/TiO_2

Samples	Band Gap Energy (eV)
MS-TiO_2	3.15
2.0 % Fe_2O_3/TiO_2	2.20
4.0 % Fe_2O_3/TiO_2	1.90

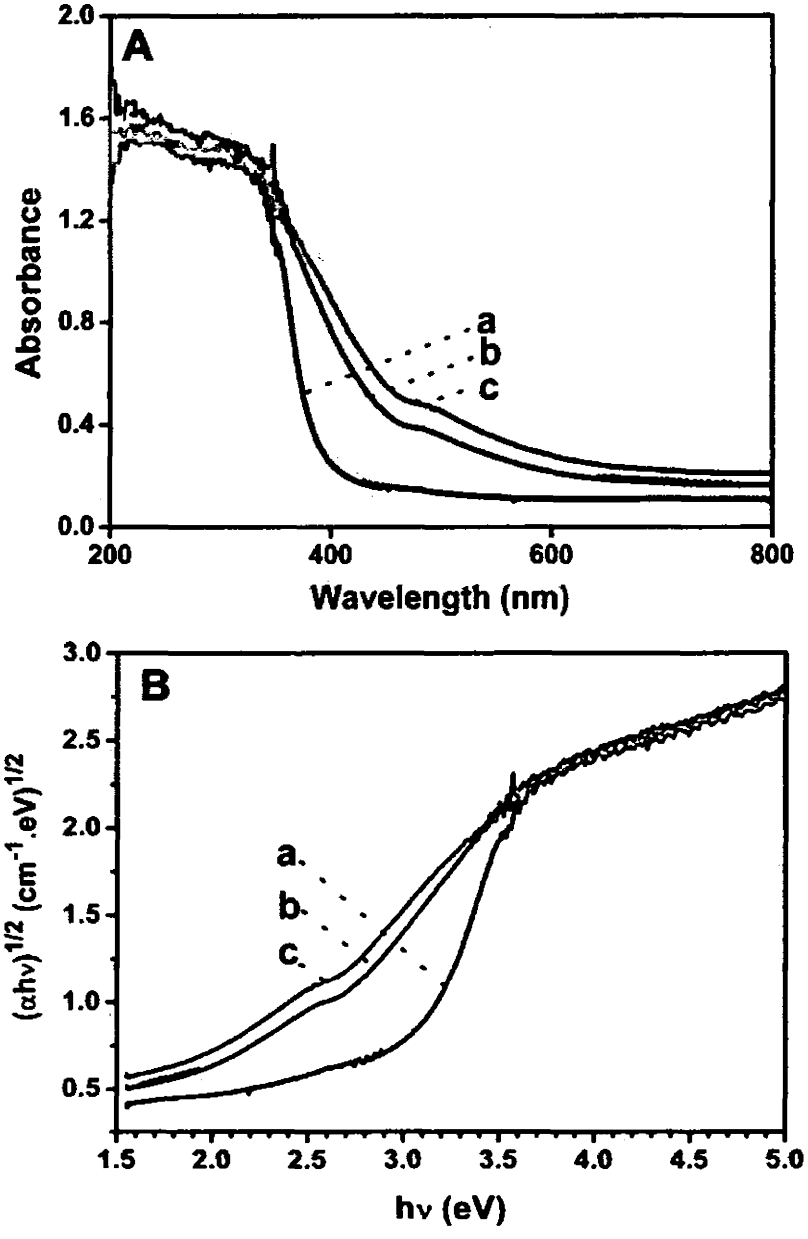

Figure 4.2. UV-vis diffused reflectance spectra of various samples (A) a plot of band gap energy of the light absorbed (B) (a) Pure TiO_2, (b) 2.0 % Fe_2O_3/TiO_2, (c) 4.0 % Fe_2O_3/TiO_2

4.3. Fourier Transform Infra-red Spectroscopy

The surface hydroxyl groups are significantly effect the photocatalytic reaction of TiO_2 which slow down the recombination of photo electrons and photo holes to make energetic molecules of oxygen. The FT-IR spectrum of Fe_2O_3, TiO_2 and 2.0 % Fe_2O_3/TiO_2 are shown in figure 4.3. Fe^{3+}ions show a peak at 1042.2 cm^{-1}, which is Fe_2O_3 characteristic peak [101]. The broad and strong peak at 1640.0 cm^{-1} is ascribed to the bending vibration for the absorption of free water and a broad peak at 3200-3600 cm^{-1} is certified the absorption of hydroxyl function group with stretch shaking, these types of groups come up from the hydrolysis progression. FT-IR study verified that group density of OH surface of pure TiO_2 is less which raises with Fe_2O_3 loading. The surface hydroxyl groups show the way for improvement in the photocatalytic activity. Since they can be able to interact with photo holes and raise the charge transferring which reduce the electron-hole pairs recombination [106].

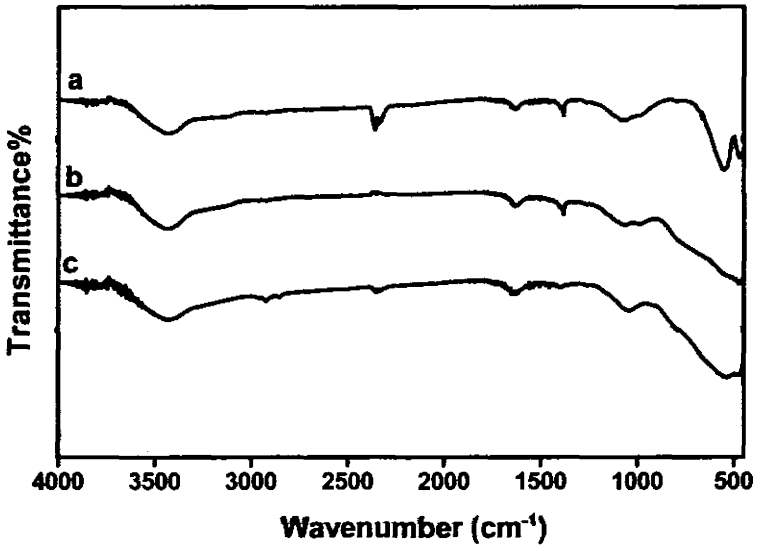

Figure 4.3. FT-IR spectra of different samples (a) Fe_2O_3, (b) TiO_2 (c) 2.0 % Fe_2O_3/TiO_2,

4.4. Scanning Electron Microscopy

Fig. 4.4 illustrates the SEM micrographs of 2.0% Fe_2O_3/TiO_2 at different magnifications. This provides the information's about the textural properties of sample indicating irregular-shaped, loose aggregates with sufficient voids between the

Particles. Addition of Fe_2O_3 has significant effect on the particle morphology and increases the level of particle aggregation in 2.0% Fe_2O_3.

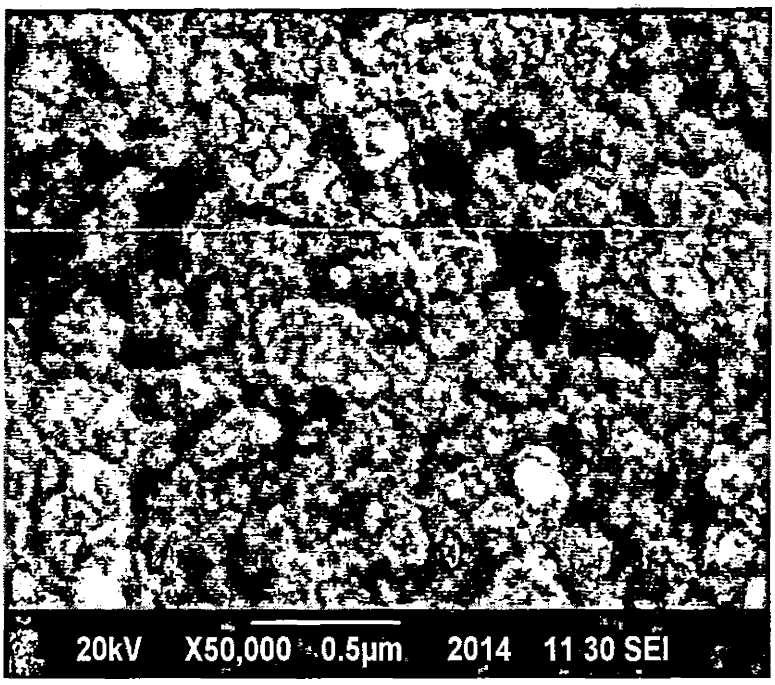

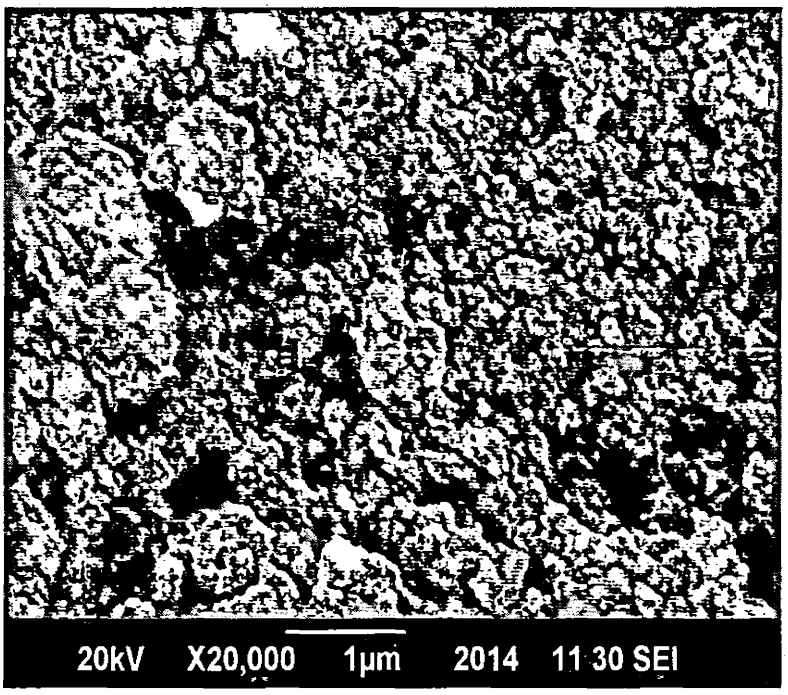

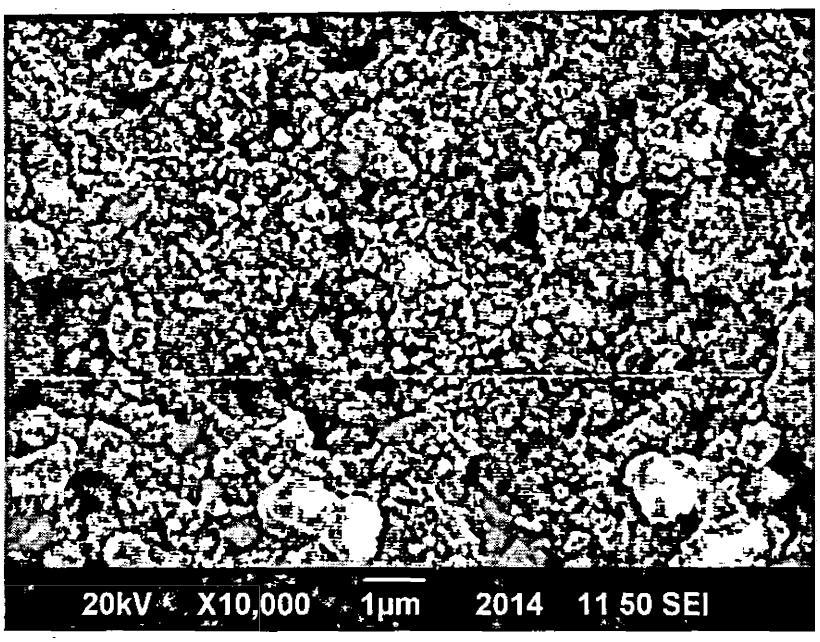

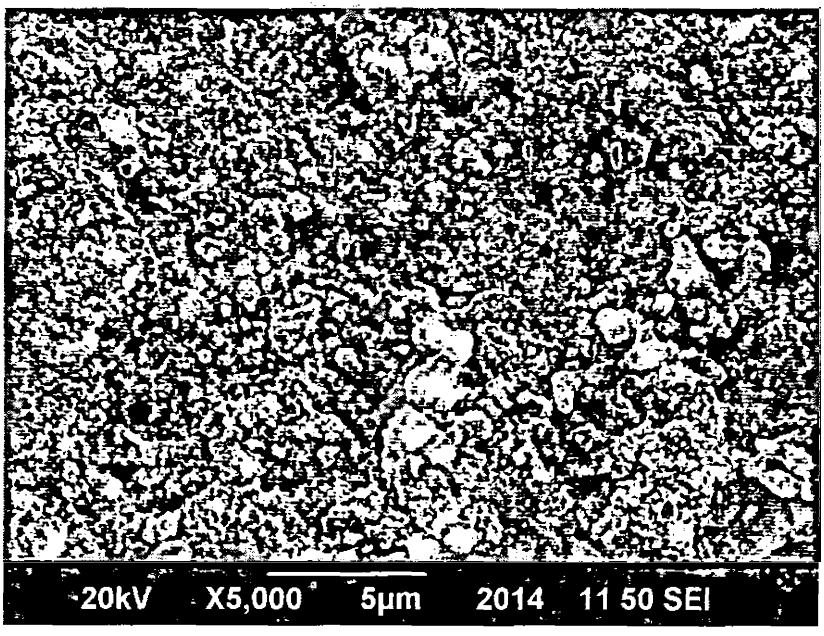

Figure 4.4 SEM images of 2.0 % Fe_2O_3/TiO_2 samples at different magnifications.

4.5. Energy Dispersive X-Ray Spectroscopy (EDXS)

Energy dispersive X-ray investigation has done to find the standard weight ratio of Fe_2O_3 to TiO_2 for 2.0 wt% Fe_2O_3/TiO_2 composite. EDX measures the surface concentration of the elements. The content of Fe_2O_3 was found to be 2.1 wt%. which

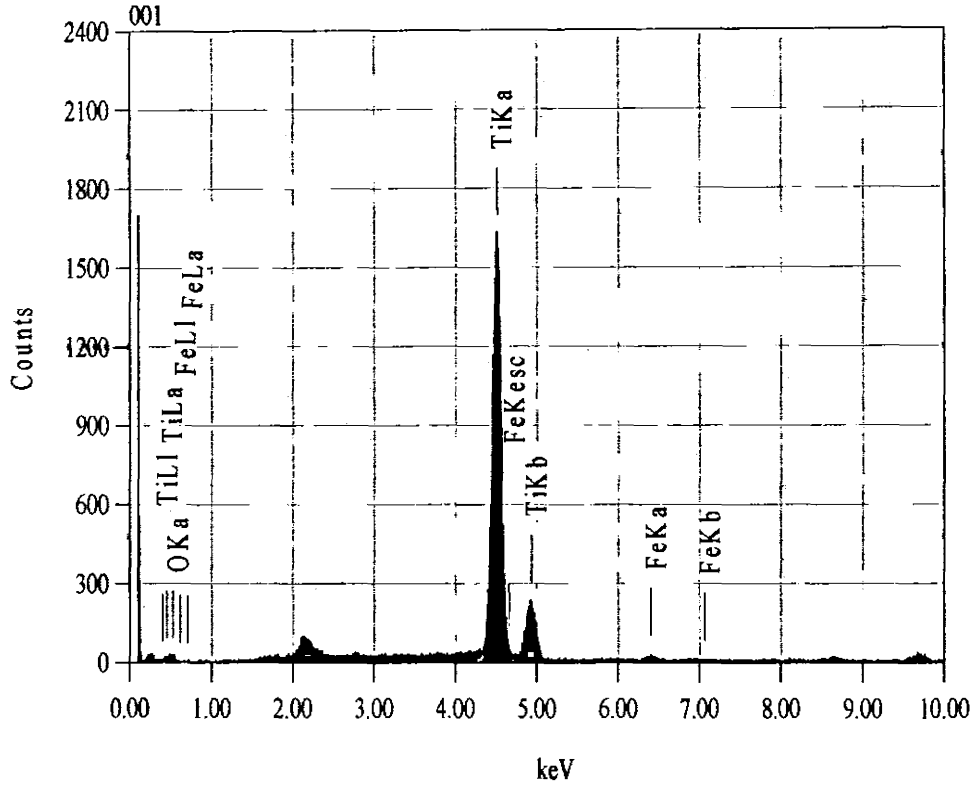

Figure 4.5. Energy dispersive X-ray analysis of 2.0 % Fe_2O_3/TiO_2

is close to its stoichiometry of 2.0 wt%. This indicates that the iron is located on the surface of the catalyst thus forming a heterojunction. The EDX spectrum of 2.0% Fe_2O_3 /TiO_2 nanocomposite is shown in figure 4.5. Clearly seen peaks of Fe, Ti and O show that nanocomposite comprises Ti, Fe and O elements. The occurrence of Au can be recognized by the Au grid. Table 4.2 illustrates the quantitative analysis of 2.0 wt% Fe_2O_3/TiO_2 composite.

Table 4.2. Quantitative analysis of 2.0 % Fe_2O_3/TiO_2 by EDX

Elements	KeV	Mass (%)	Atom (%)
O K	0.525	10.43	25.92
Ti K	4.508	87.45	72.57
Fe K	6.398	2.12	1.51

4.6. Transmission Electron Microscopy

Transmission electron microscopy (TEM) images of the 2.0 % Fe_2O_3/TiO_2 are shown in figure 4.6 reveal the uniformity of titania particles, curved and rectangular shape of anatase particles having pores in interstitial spaces and anatase crystal size is within the 15-18 nm domain (Table 4.3). These results match with the particle size (ca. 15-18 nm) find from XRD. Such type of disordered structure is produced due to interactions between the template of mesopore and titanium source. The multivalent Ti type can correlated preferably with the PEO (hydrophilic polyethylene oxide) moieties with PEG mediated to form crown-ether type complexes through coordination bonds. The resulting complexes are self assembled according to mesoscopic order and primarily bounded the micro phase separation of the block copolymer group. During hydrolysis and condensation processes, if a self-assembly of a larger Ti cluster or oligomer is produced and connected with a PEO section would be blocked systematically. This is the reverse action of forming the arranged mesostructure. Figure 4.6 showed that lattice fringes are present and clearly resolved which demonstrate that the mesopores framework is a composition of anatase nanocrystals. Thus, TEM and XRD images clearly showed that mesopore system with a well crystalline structure was present.

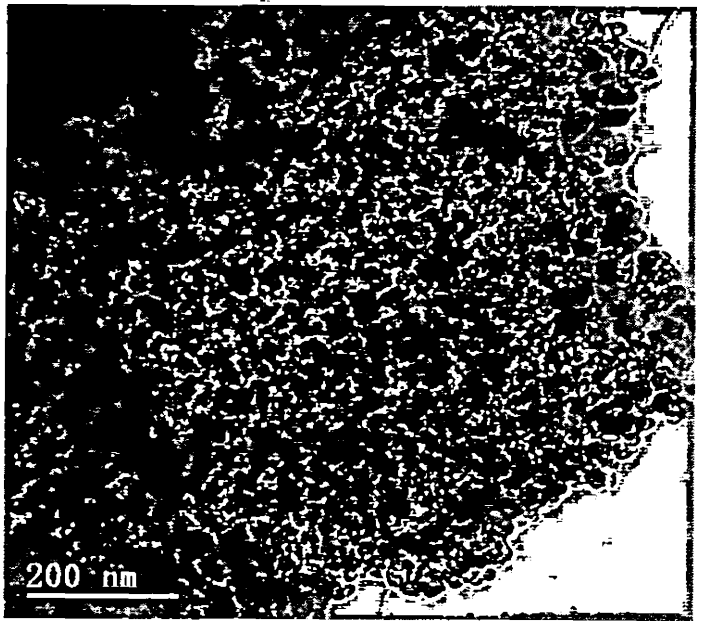

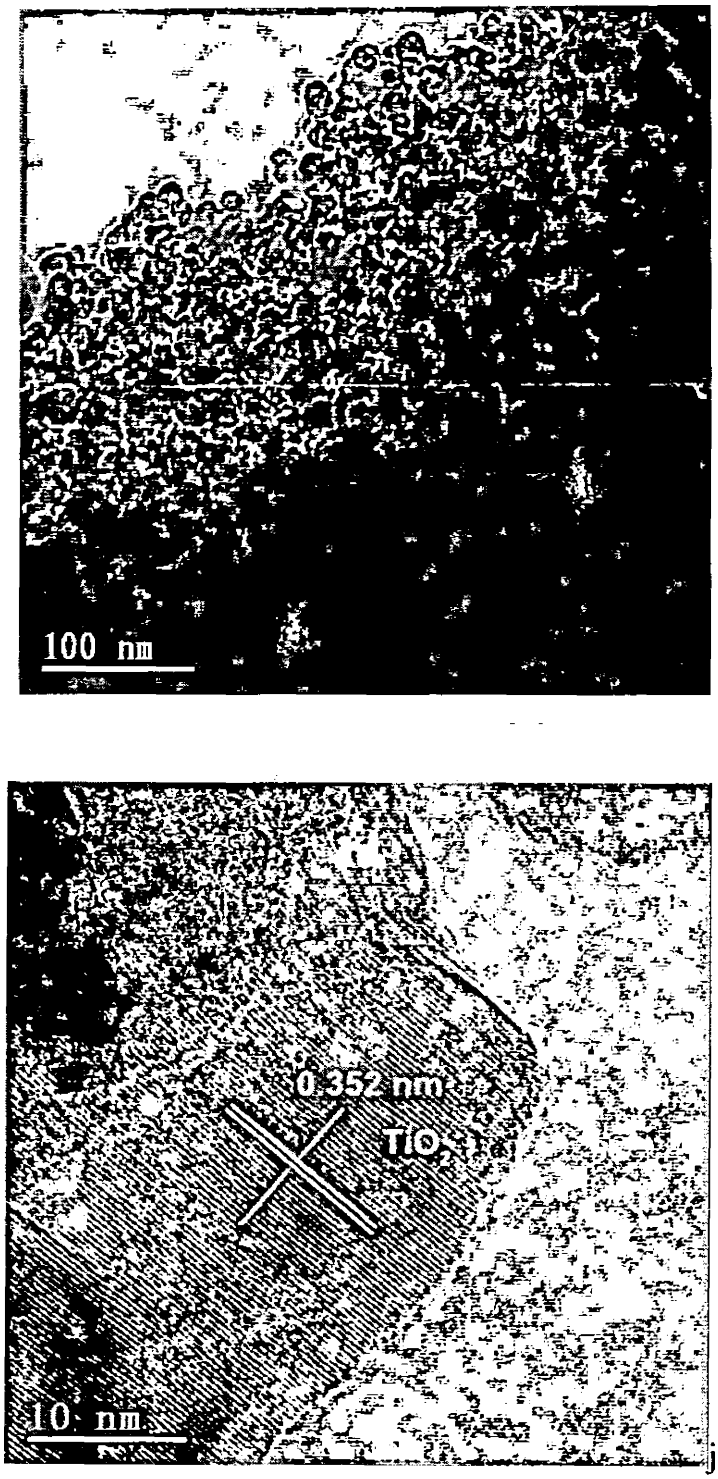

Figure 4.6. TEM and HRTEM images of 2.0 % Fe_2O_3/TiO_2 composite.

4.7. N_2 sorption data.

The distributions of pore size and isotherms of N_2 sorption mesoporous Fe_2O_3/TiO_2 composite is given in Figure 4.7. The isotherm shows that the shape of

adsorption /desorption is just like a Type IV with a H_2 hysteresis loop, at comparative high pressure of the range of 0.8 showing the huge quantity of large mesopores in samples [107]. By using PEG, 11.3 nm pore sizes of mesoporous TiO_2 were calculated.

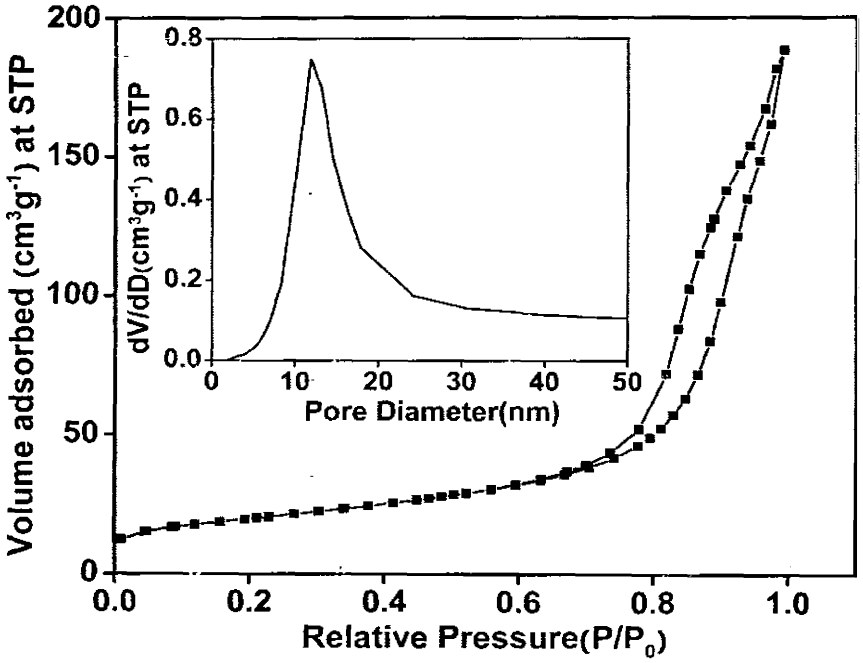

Figure 4.7. N_2 sorption isotherms of mesoporous 2.0 % Fe_2O_3/TiO_2 composite.

Table 4.3 Particle Size and Surface Area of TiO_2

Samples	Particle Size[a] (nm)	Surface Area[b] (m^2g^{-1})
MS-TiO_2	18.0	----
2.0% Fe_2O_3/ TiO_2	16.0	104
4.0% Fe_2O_3/ TiO_2	15.0	----

[a]Calculated by the Scherrer equation.

[b]BET surface area calculated from the linear part of the BET plot.

4.8. Photocatalytic activity and conductivity measurements of Fe_2O_3/TiO_2 nanocomposites

The photo catalytic performance of Fe_2O_3/TiO_2 nanocomposites was calculated during the degradation of MO. The photo catalytic degradation processes was studied under the irradiations of visible light. The photo activities for MO in presence and absence of the photo catalyst under dark and visible light irradiation respectively were also evaluated. It was found that there was no degradation for the MO in the dark and in the presence of the photo catalyst. Also no degradation was observed for MO when the solution was placed under visible light radiation without the addition of photo catalyst powder. As shown in figure 4.8, 2.0% Fe_2O_3/TiO_2 degraded 68.0% MO while the degradation pure mesoporous TiO_2 is 10.0% and degradation of Degussa P25 is 5.0% in visible light.

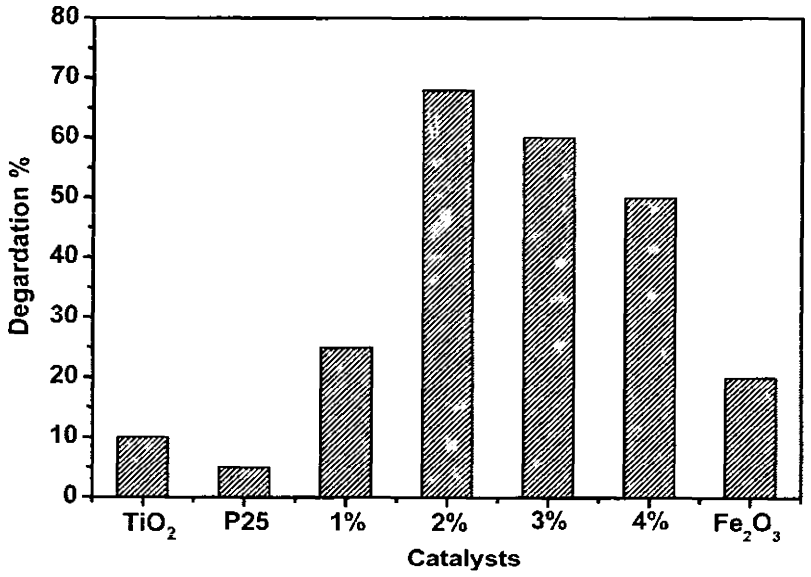

Figure 4.8. Degradation profile of MO over different photocatalysts

Photocatalytic activity of modified TiO_2 loading with 2.0% Fe_2O_3 was unexpected raise as compared to pure Degussa P25 owing to the Fe_2O_3 photosensitization is shown in figure 4.9, the transmission of reactant molecules was completed by the mesoporous channels and also they provide the bigger surface area

for Fe_2O_3 distribution. Red-shift was occur in 2.0% Fe_2O_3 loaded mesoporous TiO_2 within the absorption wavelength range and decrease the electron-hole pairs recombination rate[108].

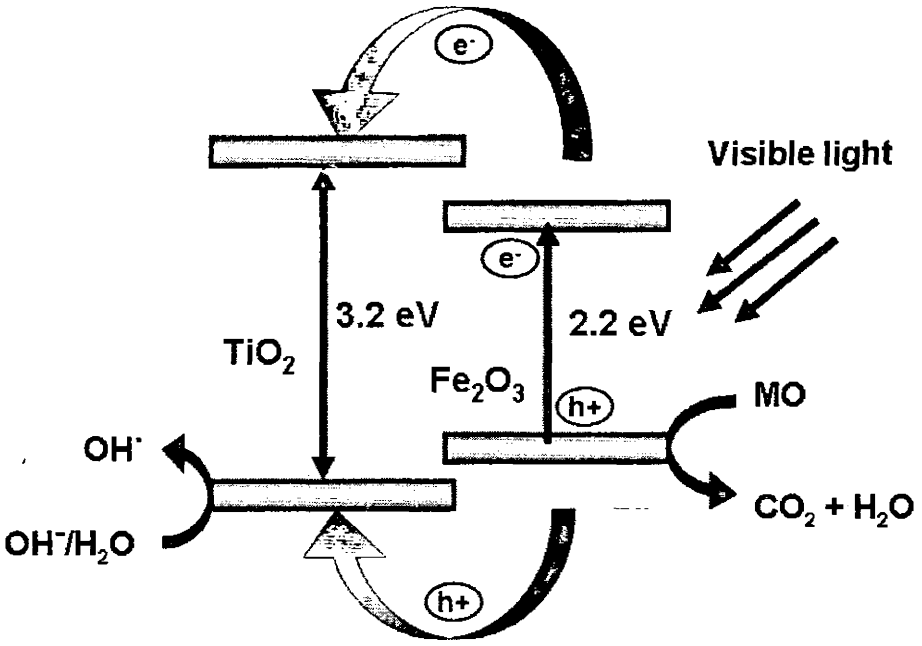

Figure 4.9 Mechanism of degradation of MO over Fe_2O_3/TiO_2.

On one hand, the lower dispersion of Fe_2O_3 reduced the end results of photosensitizing, which is the major cause of poor harvesting for visible lights. On the other hand, the higher concentration of Fe_2O_3 particles resulted in limited obstruction of mesoporous channels which can slow down the dispersion due to mesoporous channels of the reactant molecules which also make easy the reactant molecules dispersion. The space charge area reduces and becomes very narrow when ions loading concentration is high which significantly increase the diffusion penetration of light in the TiO_2 space charge layer. As a result, in a semiconductor, it is easy for photo generated electron and hole to recombine. The quick movement of photoelectrons from bulk to the surface would become easy due to the crystallization of anatase , which might effectively slow down the photoelectrons and holes recombination, the major factor to improve quantum effectiveness.

4.9 Kinetics of Reaction

Langmuir–Hinshelwood model was used to explain the kinetics of the MO photo degradation reaction. The apparent rate constant (k_{app}) is the essential kinetic factor for different photocatalysts because it determines a photocatalytic activity would not dependent on the previous adsorption phase in dark and the remaining solute concentration in the solution. The calculated apparent rate constant (k_{app}) data for Fe_2O_3/TiO_2 composite samples is enhanced by incorporating TiO_2 with Fe_2O_3. Figure 4.10 showed the experimental data, which was fit in first order kinetic equation.

$$\ln (C_o/C) = k_{app}t$$

where C = concentration of solute remaining in the solution at irradiation time of t, C_0 = initial concentration at t = 0.

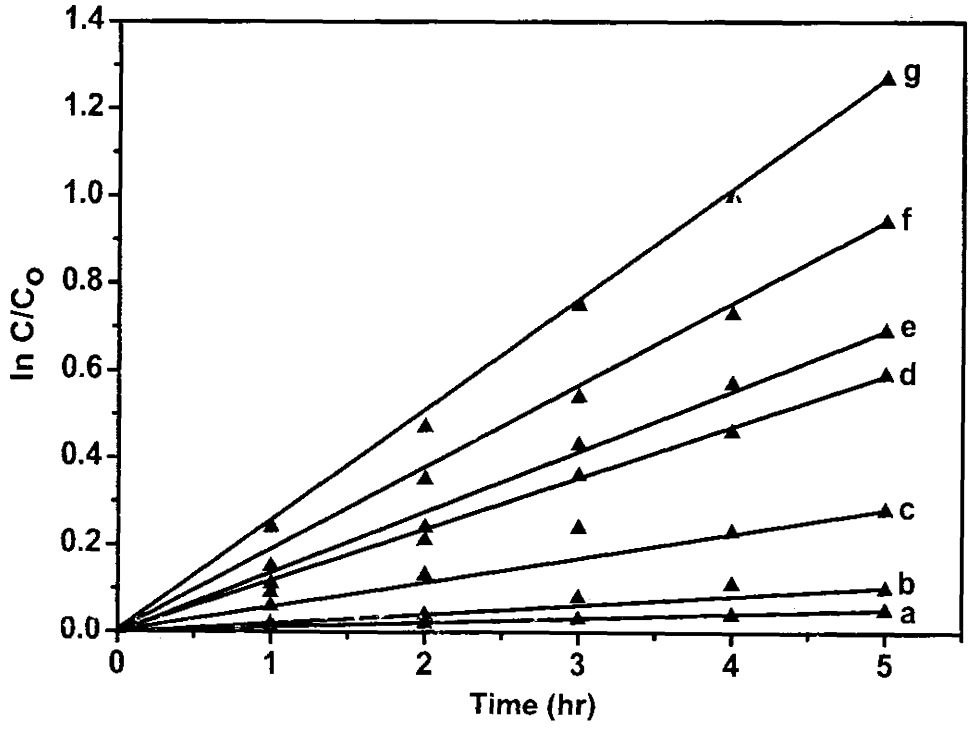

Figure 4.10. Study of Kinetic in the duration of MO degradation on (a) P-25, (b) Fe_2O_3 (c) TiO_2 (d) 1.0 % Fe_2O_3/TiO_2, (e) 4.0 % Fe_2O_3/TiO_2, (f) 3.0 % Fe_2O_3/TiO_2, (g) 2.0 % Fe_2O_3/TiO_2.

4.10 Measurement of Conductivities

The conductivities of solutions are measured by the DENVER Instrument Model 250 pH ISE conductivity meter. The electrode used for conductivity meter is K25/DENVER k=0.547@25C. The conductivities of pure Fe_3O_4, TiO_2 and different Fe_3O_4/TiO_2 composites are given in Table 4.4. The repetitive measurements were made for the catalysts and the experimental error was found within ±0.3%.

Table 4.4. The conductivities of Fe_2O_3, TiO_2 and different Fe_2O_3/TiO_2 composites.

Samples	Conductance
Ms-TiO_2	16.0 µS/cm
2.0% Fe_2O_3/ TiO_2	1.04 mS/cm
4.0% Fe_2O_3/ TiO_2	30.4 µS/cm
Fe_2O_3	18.4 µS/cm

4.11 Conclusions

Mesoporous TiO_2 was successfully prepared by a template method using tetrabutyl titanate as precursor and PEG (2000) as template. The prepared mesoporous TiO_2 was impregnated with Fe_2O_3 in different weight ratios. The loading of TiO_2 resulted into shift of absorption band to the visible region and reduced the electron hole recombination which is determining factors of the higher photo catalytic efficiencies of the catalysts. Mesoporous channels also provide more accessible sites for the diffusion of reacting species. The photo catalytic activites of the Fe_2O_3/TiO_2 were evaluated with methyl orange in comparison to P-25, pure TiO_2 and Fe_2O_3 under visible light. Kinetic studies of the photo catalytic degradation were performed and photo degradation mechanism of Fe_2O_3/TiO_2 composite has been proposed. 2.0 wt% showed superior photo catalytic activity and conductivity due to the photosensitization.

CHAPTER - 05

References:

[1] N. Taniguchi, "On the Basic Concept of 'Nano-Technology'," Proc. Intl. Conf. Prod. Eng. Tokyo, Part II, Japan Society of Precision Engineering, 1974.

[2] J.O.Carneiro, V. Teixeira, A.Portinhaet al.,"Iron-doped photocatalytic TiO_2 sputtered coatings on plastics for self-cleaning applications," Materials Science and Engineering B, vol. 138, no. 2, pp. 144–150, 2007.

[3] H. Lachheb, E. Puzenat, A. Houas et al., "Photocatalytic degradation of various types of dyes (Alizarin S, Crocein Orange G, Methyl Red, Congo Red, Methylene Blue) in water by UV-irradiated titania," Applied Catalysis B, vol. 39, no. 1, pp. 75–90, 2002.

[4] H. Zhang, H.Liu, C. Mu, C. Qiu, and D.Wu, "Antibacterial properties of nanometer Fe^{3+}-TiO_2 thin films." In proceeding of Ist IEEE international Conferenceon Nano Micro Engineered and Molecular System, pp. 955-958, 2006.

[5] H. Yu, K. Zhang, and C. Rossi, "Experimental study of the photocatalytic degradation of formaldehyde in indoor air using a nano-particulate titanium dioxide photocatalyst," Indoor and Built Environment, vol. 16, no. 6, pp. 529–537, 2007.

[6] R.Rella,J. Spadavecchia,M. G. Manera etal., "Acetone and ethanol solid-state gas sensors based on TiO_2 nanoparticles thin film deposited by matrix assisted pulsed laser evaporation," Sensors and Actuators B, vol. 127, no. 2, pp. 426–431, 2007.

[7] H. S. Jung, J. K. Lee, M. Nastasi et al., "Preparation of nanoporous MgO-coated TiO_2 nanoparticles and their application to the electrode of dye-sensitized solar cells," Langmuir, vol. 21, no. 23, pp. 10332–10335, 2005.

[8] M.R. Hoffmann, S. T. Martin, W. Choi, and D. W. Bahnemann, Environmental applications of semiconductor photo-catalysis," ChemicalReviews, vol. 95, no. 1, pp. 69–96, 1995.

[9] Fujishima, A. & Honda, K. (1972). "Electrochemical photolysis of water at a semiconductor electrode nature," Nature (London), vol. 238, pp. 37.

[10] Frank SN, Brad AJ. Hetrogenous photo catalytic oxidation of cyanide ion in aqueous solutions at titanium dioxide powder. J Am Chem Soc 1977; 99; 303

[11] Linsebigler AL, Lu G, Yater JT Jr, Photocatalysis on TiO_2 surfaces: principles, mechanisms, and selected results, Chem. Rev. 95 (1995) 735-758.

[12] Mills A, Le Hunte S, An overview of semiconductor photocatalysis, J. Photochem. Photobiol. A: Chemistry 108 (1997) 1-35.

[13] Sreethawong T, Suzuki Y, Yoshikawa S, Synthesis, characterization, and photocatalytic activity for hydrogen evolution of nanocrystalline mesoporous titania prepared by surfactant-assisted templating sol–gel process, J. Solid. State Chem. 178/1 (2005) 329-338.

[14] Shaban YA, Khan SUM, Visible light active carbon modified n- TiO_2 for efficient hydrogen production by photoelectrochemical splitting of water, Int. J. Hydrogen Energy 33/4 (2008) 1118-1126.

[15] Tian-Hua Xu, Chen-Lu Song, Yong Liu, and Gao-Rong Han, Band structures of TiO_2 doped with N, C and B; J Zhejiang Univ Sci B.7(4) (2006)

[16] Naicker , P.K., Cummings , P.T. et al. (2005) Characterization of titanium dioxide nanoparticles using molecular dynamics simulations . Journal of Chemistry B, 109 (32), 15243–9 .

[17] M. Schmidt, E. Fehling, C. Glotzbach, S. Fröhlich, S. Pietrowski, Eds., Ultrahigh performance concrete and nanotechnology in construction, Kassel University Press Kassel, 2012, 177-184.

[18] Li G, Chen L, Graham M E, et al. A comparison of mixed phase titania photocatalysts prepared by physical and chemical methods: The

importance of the solid-solid interface. J Mol Catal A Chem, 2007, 275: p-30

[19] Xu, Y. & Schoonen, M. (2000). "The absolute positions of conduction and valence bands of selected semiconducting materials," American Mineralogist, vol. 85, pp. 543- 556

[20] Blake, D. (1999). "Bibliography of work on the heterogeneous photo catalytic removal of hazardous compounds from water and air," National Renewal Energy Laboratory

[21] Yang , H.M., Shi , R.R. et al . (2005) Synthesis of WO_3/TiO_2 nanocomposites via sol - gel method . Journal of Alloys and Compounds, 398 (1 – 2), 200–2 .

[22] Rajh , T., Chen , L.X. et al . (2002) Surface restructuring of nanoparticles: an efficient route for ligand - metal oxide crosstalk . Journal of Physical Chemistry B, 106 (41), 10543–52 .

[23] Gratzel , M. (2004) Conversion of sunlight to electric power by nanocrystalline dye - sensitized solar cells . Journal of Photochemistry and Photobiology A: Chemistry, 164, 3–14 .

[24] Cozzoli , P.D., Fanizza , E. et al . (2004) Role of metal nanoparticles in TiO_2/Ag nanocomposite - based microheterogeneous photocatalysis . Journal of Physical Chemistry B, 108 (28), 9623–30 .

[25] Li , G.H. and Gray , K.A. (2007) The solid - solid interface: explaining the high and unique photocatalytic reactivity of TiO_2 - based nanocomposite materials . Chemical Physics, 339, 173–87 .

[26] Yu , J.G., Xiong , J.F. et al . (2005) Fabrication and characterization of Ag - TiO_2 multiphase nanocomposite thin films with enhanced photocatalytic References activity. Applied Catal; B: Environmental, 60 (3 – 4), 211–21 .

[27] Yu , J.G., Yue , L. et al . (2009) Hydrothermal preparation and photocatalytic activity of mesoporous Au - TiO_2 nanocomposite microspheres . Journal of Colloid and Interface Science.

[28] Szacilowski K, Macyk W, Drzewiecka-Matuszek A, et al. Bioinorganic photochemistry: Frontiers and mechanisms. Chem Rev, 2005, photoactivity. 105: 2647–2694

[29] Grätzel M, Howe R F. Electron paramagnetic resonance studies of doped TiO_2 colloids. J Phys Chem, 1990, 94: 2566–2572

[30] Choi Y, Termin A, Hoffmann M R. The role of metal ion dopants in quantum-sized TiO_2: Correlation between photoreactivity and charge carrier recombination dynamics. J Phys Chem, 1994, 98: 13669– 13679

[31] Joshi M M, Labhsetwar N K, Mangrulkar P A, et al. Visible light induced photoreduction of methyl orange by N-doped mesoporous titania. App Catal A General, 2009, 357: 26–33

[32] Maruska H P, Ghosh A K. Transition-metal dopants for extending the response of titanate photoelectrolysis anodes. Sol Energy Mater, 1979, 1: 237

[33] Gautron J, Lemasson P, Marucco J M. Correlation between the non-stoichiometry of titanium dioxide and its behaviour. Faraday Discuss Chem Soc, 1981, 70: 81–91

[34] Fox M A, Dulay M T. Heterogeneous photocatalysis. Che. Rev, 1995, 93:341

[35] Xin B, Ren Z, Wang P, et al. Study on the mechanisms of photoinduced carriers separation and recombination for Fe^{3+}- TiO_2 catalysts. App Surf Sci, 2007, 253: 4390–4395

[36] Li R, Chen W, Wang W. Magnetoswitchable controlled photocatalytic system using ferromagnetic Fe-doped titania nanorods photocatalysts with enhanced photoactivity. Sep Purif Technol, 2009, 66: 171–176

[37] Periyasami V, Chinnathambi M, Chinnathambi S, et al. Photocatalytic activity of iron doped nanocrystalline titania for the oxidative degradation of 2,4,6-trichlorophenol. Catal Today, 2009, 141: 220–224

[38] Khan M A, Han D H, Yang O B. Enhanced photoresponse towards visible light in Ru doped titania nanotube. Appl Surf Sci, 2009, 255: 3687–3690

[39] Prasad G K, Singh B, Ganesan K, et al. Modified titania nanotubes for decontamination of sulpher mustard. J Hazard Mater, 2009, 167: 1192–1197

[40] El-Bahy Z M, Ismail A A, Mohamed R M. Enhancement of titania by doping rare earth for photodegradation of organic dye (Direct blue). J Hazard Mater, 2009, 166: 138–143

[41] Wang C, Ao Y, Wang P, et al. Photocatalytic performance of Gd ion modified titania porous hollow spheres under visible light. Mat Lett, 2010, 64: 1003–1006

[42] Wang C, Ao Y, Wang P, et al. Preparation, characterization, photo catalytic properties of titania hollow doped with cerium. J Hazard Mater, 2010, 178: 517–521.

[43] A.K.L. Sajjad, S. Shamaila, B. Tian, F. Chen, J. Zhang, One step activation of WO_x/TiO_2 nanocomposites with enhanced photo catalytic activity. Appl. Catal. B Environ. 91 (2009) 397- 405.

[44] Asahi R, Morikawa T, Ohwaki T, et al. Visible-light photocatalysis in nitrogen-doped titanium oxides. Science, 293: 269–271

[45] Diwald O, Thompson T L, Goralski E G, et al. The effect of nitrogen ion implantation on the photoactivity of TiO_2 rutile single crystals. J Phys Chem B, 2004, 108: 52–57

[46] Ao Y, Xu J, Zhang S, et al. A one-pot method to prepare N-doped titania hollow spheres with high photocatalytic activity under visible light. Appl Surf Sci, 2010, 256: 2754–2758

[47] Dong L, Cao G X, Ma Y, et al. Enhanced photocatalytic degradation properties of nitrogen-doped titania nanotube arrays. Trans Nonferrous Met Soc China, 2009, 19: 1583–1587

[48] Yu J C, Yu J G, Ho W K, et al. Effects of F doping on the photocatalytic activity and microstructures of nanocrystalline TiO_2 powder. Chem Rev, Chem Mater, 2002, 14: 3808–3816

[49] Sakthivel S, Kisch H. Daylight photocatalysis by carbon-modified titanium dioxide. Angrew Chem Int Ed, 2003, 42: 4908–4911

[50] Park J H, Kim S, Bard A J. Novel carbon-doped TiO_2 nanotube arrays with high aspect ratios for efficient solar water splitting. Nano Lett, 2006, 6: 24–28

[51] A.K.L. Sajjad, S. Shamaila, B. Tian, F. Chen, J. Zhang, Comparative studies of operational parameters of degradation of azo dyes in visible light by highly efficient WO_x/TiO_2 photocatalyst. J. Hazard. Mater. 177 (2010) p-781

[52] A.K.L. Sajjad, S. Shamaila, F. Chen, J. Zhang, WO_3/TiO_2 composite with morphology change via hydrothermal template-free route as an efficient visible light photo catalyst. Chem. Eng. J. 166 (2011) 906-915.

[53] S. Shamaila, A.K.L. Sajjad, F. Chen, J. Zhang, WO_3/BiOCl a novel heterojunction as visible light photocatalyst, J. Colloids Interface Sci. 356 (2011) 465-472

[54] J. Zhang, Y. Wu, M. Xing, A.K.L. Sajjad, S. Shamaila, Development of modified N doped TiO_2 photocatalyst with metals, nonmetals and metal oxides. A review; Energy Environ. Sci. 3 (2010) 715 –726.

[55] Yang P, Lu C, Hua N, et al. Titanium dioxide nanoparticles co-doped with Fe^{3+} and Eu^{3+} ions for photocatalysis. Mater Lett, 2002, 57: 794–801

[56] Vasiliu F, Diamandescu L, Macovei D, et al. Fe-and Eu-doped TiO_2 photocatalytical materials prepared by high energy ball milling. Top Catal, 2009, 52: 544–556

[57] Song K, Zhou J, Bao J, et al. Photocatalytic activity of (copper, nitrogen)-codoped titanium dioxide nanoparticles. J Am Ceram Soc, 2008, 91: 1369–1371

[58] Xu J, Ao Y, Fu D. A novel Ce, C-codoped TiO_2 nanoparticles and its photocatalytic activity under visible light. Appl Surf Sci, 2009, 256: 884–888

[59] Shen X Z, Liu Z C, Xie S M, et al. Degradation of nitrobenzene using titania photocatalyst co-doped with nitrogen and cerium under visible light illumination. J Hazard Mater, 2009, 162: 1193–1198

[60] Zhu , J.H. , Yang , D. et al . (2008)Synthesis and characterization ofbamboo - like CdS/TiO 2 nanotubescomposites with enhanced visible – light photocatalytic activity . Journal of Nanoparticle Research , 10 (5), 729 – 36 .

[61] Xiao , M.W. , Wang , L.S. et al . (2009)Synthesis and characterization of WO 3 /titanate nanotubes nanocomposite withenhanced photocatalytic properties .Journal of Alloys and Compounds , 470(1 – 2), 486 – 91 .

[62] Yu , M.D. , Guo , Y. et al . (2008) A novelpreparation of mesoporous Cs x H 3 –x PW 12 O 40 /TiO 2 nanocomposites withenhanced photocatalytic activity . colloids and Surfaces A: Physicochemical andEngineering Aspects , 316 (1 – 3), 110 – 18 .

[63] Li , S.Y. , Chen , M.K. et al . (2009)Preparation and characterization of polypyrrole/TiO 2 nanocomposite and its photocatalytic activity under visible light irradiation . Journal of Materials Research ,24 (8), 2547 – 54 .

[64] Min , S.X. , Wan , F. *et al* . (2009) Preparation and photocatalytic activity of PANI/AMTES - TiO 2 nanocomposite materials . *A cta Physico- Chimica Sinica* ,25 (7), 1303 – 10 .

[65] Lei , S.M. , Gong , W.Q. *et al* . (2006) Preparation of TiO 2 /kaolinite nanocomposite and its photocatalytical activity . Journal of Wuhan University of Technology: Materials Science Edition , 21 (4), 12 – 15 .

[66] Luo , Y.B. , Li , W.D. *et al* . (2009) Preparation and properties of nanocomposites based on poly(lactic acid) and functionalized TiO_2 . Acta Materialia , 57 (11), 3182 – 91 .

[67] Shchukin , D. , Poznyak , S. *et al* . (2004) TiO 2 - In_2O_3 photocatalysts: reparation,characterisations and activity for 2 - chlorophenol degradation in

water. Journal of Photochemistry and Photobiology A: Chemistry , 162(2 – 3), 423 – 30 .

[68] Kun , R. , Mogyorosi , K. *et al* . (2006) Synthesis and structural and photocatalytic properties of TiO 2 /montmorillonite nanocomposites .*Applied Clay Science* , 32 (1 – 2), 99 – 110 .

[69] Carp O, Huisman C L, Reller A. Photoinduced reactivity of titanium dioxide. Prog in Solid State Chem, 2004, 32: 33–117

[70] Hagfeldtt A, Grätzel M. Light-induced redox reactions in nanocrystalline systems. Chem Rev, 1995, 95: 49–68

[71] Mills A, Hunte A J. An overview of semiconductor photocatalysis. J photochem Photobiol A Chem, 1997, 108: 1–35

[72] Bahnemann D W, Kormann C, Hoffmann M R. Preparation and characterization of quantum size zinc oxide: A detailed spectroscopic study. J Phys Chem, 1987, 91: 3789–3798

[73] Yang P., Deng T., Zhao D., Feng P., Pine D., Chmelka B. F., Whitesides G. M.,Stucky G. D., Hierarchically ordered oxides. Science 1998, 282(5397), 2244

[74] Yang P. D., Zhao D. Y., Margolese D. I., Chmelka B. F., Stucky G. D., Generalized syntheses of large-pore mesoporous metal oxides with semicrystalline frameworks. Nature 1998, 396: 152-155.

[75] Antonelli D. M., Ying J. Y., Synthesis and characterization of hexagonally packed mesoporous tantalum oxide molecular sieves. Chem. Mater. 1996, 8(4): 874.

[76] IUPAC, Pure and Applied Chemistry 1972, 31: 578.

[77] Wonyong Choi, Andreas Termin, Michael R. Hoffmann. The Role of Metal Ion Dopants in Quantum-Sized TiO_2 Correlation between Photoreactivity and Charge Carrier Recombination Dynamics *J. Phys. Chem.*, 1994, 98 (51), 13669

[78] Xin, B.F., Ren, Z.Y., Wang, P., Liu, J., Jing, L.Q., Fu, H.G. Study on the mechanisms of photoinduced carriers separation and recombination for Fe^{3+}–TiO_2 photocatalysts Appl. Surf. Sci., 007, 253, 4390.

[79] Adán, C., Bahamonde, A., Fernández-Garcia, M., A.Martinez-Arias: Structure and activity of nanosized iron-doped anatase TiO_2 catalysts for phenol photocatalytic degradation Appl. Catal. B, 2007, 72,11.

[80] Klosek and Daniel Raftery Visible Light Driven V-Doped TiO_2 Photocatalyst and Its Photooxidation of Ethanol *J. Phys. Chem. B*, 2001, 105 (14), 2815

[81] Zhu, J.F., Deng, Z.G., Chen, F., Zhang, J.L., Chen, H.J., Anpo, M., Huang, J.Z., L.Z. Zhang, Hydrothermal doping method for preparation of Cr^{3+}-TiO_2 photocatalysts with concentration gradient distribution of Cr^{3+}. Appl. Catal. B, 2006, 62, 329.

[82] Lam, R.C.W., Leung, M.K.H., Leung, D.Y.C., Vrijmoed, L.L.P., Yam W.C., Ng, S.P. Vissible-light assisted photo catalytic degradation of gaseous for maldehyde by parallel palte reactor coated with Cr-ion implated TiO_2 thin film. Sol. Energ. Mat. Sol. C, 2007, 91, 54.

[83] Venkatachalam, N., Palanichamy, M., Arabindoo, B. Murugesan, V. J. Synthesis and characterization of Zr^{4+}, La^{3+} and Ce^{3+}doped mesoporous TiO_2: Evaluation of their photocatalytic activityMol. Catal. A, 2007, 266, 158.

[84] Paola, A.D., Garcia-López, E., Ikeda, S., Marci, G., Ohtani, B., Palmisano, L. Catal. Today, 2002, 75, 87.

[85] Dvoranová, D., Brezová, V.,.Mazŭr, M, Malati M.A. Investigations of metal-doped titanium dioxide photocatalystsAppl. Catal. B, 2002, 37, 91.

[86] Brezovó, V., Bla·zkovó, A.,.Karpinskŷ, Lo, Gro·sková, J., Havlinová, B., Jorik, V., J. M., Phenol decomposition using M^{n+}/TiO_2 photocatalysts supported by the sol-gel technique on glass fibres Photochem. Ceppan: Photobiol. A, 1997, 109, 177.

[87] Bouras, P., Stathatos, E., Lianos P. Pure versus metal-ion-doped

nanocrystalline titania for photocatalysis Appl. Catal. B, 2007, 73, 51.

[88] Anpo, M. Takeuchi, M., Ikeue, K. Dohshi, S. Curr. Opin. Solid State Mater. Sci., 2002, 6, 381.

[89] Anpo, M., Takeuchi ,M. J. Catal., 2003, 216, 505.

[90] Anpo, M., Takeuchi, M. Int. J. Photoenergy, 2001, 3, 89.

[91] K. Nagaveni, M. S. Hegde, and Giridhar Madras Structure and photocatalytic Activity of $Ti_{1-x}M_xO_{2\pm\delta}$ (M = W, V, Ce, Zr, Fe, and Cu) Synthesized by Solution Combustion Method J. Phys. Chem. *B*, 2004, 108 (52), pp 20204–20212

[92] Casarin, M., Maccato, C., Vittadini A. Electronic structure of Nb impurities in and on TiO_2 Phys. Chem., 1999, 1, 3793.

[93] Nishikawa, T., Nakajima, T., Shinohara, Y. An exploratory study on effect of the isomorphic replacement of Ti^{4+} ions by various metal ions on the light absorption character of TiO_2. J. Mol. Struct., 2001, 545, 67.

[94] Karvinen. S., Hirva, P., Pakkanen, T.A. Ab initio quantum chemical studies of cluster model for doped anatase and rutile TiO_2. J. Mol. Strct., 2003, 626,271.

[95] Yu, J.C., Yu, J.G., Ho, W.K., Jiang, Z.T., Zhang L.Z. An exploratory study on effect of the isomorphic replacement of Ti^{4+} ions by various metal ions on the light absorption character of TiO_2 Chem. Mater., 2002, 14, 3808.

[96] Yu, J.G., Yu, J.C., Cheng, B., Hark, S.K, Iu, K. The effect of F-Dopping and temperature on the structural and textural evolution of mesoporous TiO_2 powder. J. Solid State Chem., 2003, 174, 372.

[97] Yamaki, T., Umebayashi, T., Sumita, T., Yamamoto, S., Maekawa, M., Kawasuso,A, Itoh, H, Fluorine-doping in titanium dioxide by ion implantation technique. Nucl. Inst. Methods Phys. Res Sect. B, 2003,206, 254

[98] Li Z, Shen W, He W, Zu X, Effect of Fe-doped TiO_2 nanoparticle derived From modified hydrothermal process on the photocatalytic degradation performance on methylene blue. . J Hazard Mater. 2008 155, 590-4.

[99] Othman, S., H., Abdul Rashid, S., Mohd Ghazi, T, I, Norhafizah .A. Fe-Doped TiO_2 Nanoparticles Produced via MOCVD: Synthesis, Characterization and Photocatalytic Activity, J. Nanomater. 2011

[100] Chen, X. Q., Yang J.Y., Zhang J. S., Preparation and photo catalytic properties of Fe-Doped TiO_2 nanoparticles, J. Cent. S. Uni. Tech. 2004, 11, 161-165

[101] Xing, M.Y. Zhang, J. Chen, F Photocatalytic performance of N-Doped TiO_2 adsorbed with Fe^{3+} ions under visible light by a redox treatment, J. Phy. Chem. C. 2009,11, 197-204

[102] Kokila1, P., Senthilkumar, V., Nazeer, K.P., Preparation and photo catalytic activity of Fe^{3+}doped TiO_2 nanoparticles, Archives of Phy; Research, 2011,2

[103] Shi, Z.L., Lai, H., Yao, S.H., Wang, S.F. Photocatalytic activity of Fe and Ce co-doped mesoporous TiO_2 catalyst under UV and visible light, J. Chin.Chem. Soc. 2012, *59*, 0000-0000

[104] Xu, J. C., Mei, L., Yong, X. G., Li, H. L. Zinc ions surface-doped titanium dioxide nanotubes and its photocatalysis activity for degradation of methyl orange in water. J. Mol. Catal. A: Chem., 2005, 226, 123-137.

[105] Kochkar, H., Turki, A.; Bergaoui, L.; Berhault, G.; Ghorbel, A. Study of Pd (II) adsorption over titanate nanotubes of different diameters. J. Coll. Interf. Sci., 2009, 331, 27-31

[106] Lopez, T., Moreno, J. A., Gomez, R., Bokhimi, X., Wang, J. A. Madeira, H. Y, Pecchic, G., Reyesc, P. Charecterization of Iron doped titania by sol gel materials, J. Mater. Chem., 2002, 12, 1–6

[107] Perkas, N. Wang, Y, Koltypin, Y., Gedanken, A. S., Chandrasekaran, S, Mesoporous iron–titania catalyst for cyclohexane oxidation, *Chem. Commun.*, 2001, 988–989

[108] Hussain, S. T., Siddiqa, A. Iron and chromium doped titanium dioxide, nanotubes for the degradation of environmental and industrial pollutants, Int. J. Environ. Sci. Tech., 2011, 8, 351-362.